
Asynchronous ϵ -Greedy Bayesian Optimisation

George De Ath

Richard M. Everson

Jonathan E. Fieldsend

Department of Computer Science, University of Exeter, United Kingdom

Abstract

Bayesian Optimisation (BO) is a popular surrogate model-based approach for optimising expensive black-box functions. In order to reduce optimisation wallclock time, parallel evaluation of the black-box function has been proposed. Asynchronous BO allows for a new evaluation to be started as soon as another finishes, thus maximising utilisation of evaluation workers. We present AEGiS (Asynchronous ϵ -Greedy Global Search), an asynchronous BO method that, with probability 2ϵ , performs either Thompson sampling or random selection from the approximate Pareto set trading-off between exploitation (surrogate mean prediction) and exploration (surrogate posterior variance). The remaining $1 - 2\epsilon$ of moves exploit the surrogate's mean prediction. Results on fifteen synthetic benchmark problems, three meta-surrogate hyperparameter tuning problems and two robot pushing problems show that AEGiS generally outperforms existing methods for asynchronous BO. When a single worker is available performance is no worse than BO using expected improvement. We also verify the importance of each of the three components in an ablation study, as well as comparing Pareto set selection to selection from the entire feasible problem domain, finding that the former is vastly superior.

derivative information (Snoek et al., 2012; Brochu et al., 2010). BO comprises two main steps which are repeated until convergence or the budget is exhausted. Firstly, a surrogate model is constructed using previous evaluations; this is typically a Gaussian process (GP), due to its strength in uncertainty quantification and function approximation (Shahriari et al., 2016; Rasmussen and Williams, 2006). Secondly, an acquisition function is optimised to select the next location to expensively evaluate. Such functions attempt to balance the exploitation of locations with a good predicted value with the exploration of locations with high uncertainty.

In real-world problems it is often possible to use hardware capabilities to run multiple evaluations in parallel. For example, the number of hyperparameter configurations that can be evaluated in parallel when training neural networks (Chen et al., 2018) is only limited by the computational resources available. The desire to speed up optimisation wallclock time through parallel evaluation led to the development of parallel BO in which q locations are jointly selected to be evaluated synchronously. It has been successfully applied in many areas such as drug discovery (Hernández-Lobato et al., 2017), heat treatment, (Gupta et al., 2018), and hyperparameter configuration (Kandasamy et al., 2018).

In cases where the runtime for evaluations varies, such as when optimising the number of units in the layers of a neural network, or indeed the number of layers themselves, synchronous parallel approaches will result in resource underutilisation because all evaluations must finish before the next q locations can be suggested. To counteract this, asynchronous BO approaches have been proposed that allow for the evaluation of functions asynchronously; i.e., as soon as an evaluation has completed, another can be submitted. In order to take into account the uncertainty in the surrogate model at and around locations that which are still being evaluated, a number of different *ad hoc* methods have been proposed to penalise either the surrogate model itself or the acquisition function in order to limit the selection of locations near places that are currently under evaluation (Ginsbourger et al., 2008; Gonzalez et al., 2016; Alvi et al., 2019).

1 Introduction

Bayesian Optimisation (BO) is a popular sequential approach for optimising time-consuming or costly black-box functions that have no closed-form expression or

Kandasamy et al. (2018) presented an alternative approach based on Thompson sampling (TS) that draws function realisations from the GP posterior and optimises these to suggest new locations to evaluate without the need to penalise the model or acquisition function. However, TS relies on there being enough stochasticity to create sufficiently diverse function draws with meaningfully different optima. Therefore, TS tends to be insufficiently exploratory in low dimensions (as draws are very similar to the mean prediction) and over-exploratory in high dimensions where the posterior uncertainty is high across much of the domain.

ϵ -greedy methods have been shown to be remarkably successful in sequential and synchronous parallel optimisation (De Ath et al., 2020; De Ath et al., 2020). Most of the time these exploit the mean prediction of the surrogate model by expensively evaluating the location with the best posterior mean, ignoring the uncertainty in the surrogate’s prediction, but making deliberately exploratory samples with probability ϵ . In this work we combine a greedy exploitation of the mean prediction with Thompson sampling and random selection from the approximate Pareto set that maximally trades off exploration and exploitation. Specifically, we introduce an ϵ -greedy scheme that, with probability 2ϵ performs either Thompson sampling or random selection from the approximate Pareto set, and exploits the surrogate model’s posterior mean prediction the rest of the time, i.e. with probability $1 - 2\epsilon$. One of the reasons for the success of ϵ -greedy methods is that model inaccuracy introduces some accidental exploration even when exploiting the mean prediction. This effect becomes dominant as the dimension increases, and we therefore investigate how ϵ can be reduced with increasing dimension.

- We present AEGiS (Asynchronous ϵ -Greedy Global Search), a novel asynchronous BO algorithm that combines greedy exploitation of the posterior mean prediction with Thompson sampling and random selection from the approximate Pareto set between exploration and exploitation.
- We present results on fifteen well-known benchmark functions, three meta-surrogate hyperparameter tuning problems and two robot pushing problems. Empirically, we demonstrate that AEGiS outperforms existing methods for asynchronous BO on synthetic and hyperparameter optimisation problems.
- We investigate how the degree of deliberate exploration ϵ should be controlled with increasing dimension, d , showing empirically that $\epsilon = \min(1/\sqrt{d}, 1/2)$ yields good performance over a range of problems.
- We present an ablation study that highlights the

importance of all three components, i.e. the Pareto set selection, Thompson sampling, and exploitation.

We begin in Section 2 by reviewing sequential, synchronous and asynchronous BO, and Thompson sampling, before introducing AEGiS in Section 3. Section 4 details extensive empirical evaluation of AEGiS against other popular methods on well-known test problems, and also includes an ablation study. We finish with concluding remarks in Section 5.

2 Bayesian Optimisation

Our goal is to minimise a black-box function $f : \mathcal{X} \mapsto \mathbb{R}$, defined on a compact domain $\mathcal{X} \subset \mathbb{R}^d$. The function itself is unknown, but we have access to the result of its evaluation $f(\mathbf{x})$ at any location $\mathbf{x} \in \mathcal{X}$. We are particularly interested in cases where the evaluations are expensive, either in terms of time or money or both. We therefore seek to minimise f in either as few evaluations as possible to incur as little cost as possible or for a fixed budget.

2.1 Sequential Bayesian Optimisation

Bayesian Optimisation (BO) is a global search strategy that sequentially samples the problem domain \mathcal{X} at locations that are likely to contain the global optimum, taking into account both the predictions of a probabilistic surrogate model and its corresponding uncertainty (Jones et al., 1998). It starts by generating M initial sample locations $\{\mathbf{x}_i\}_{i=1}^M$ with a space filling algorithm, such as Latin hypercube sampling (McKay et al., 1979), and expensively evaluates them with the function $f_i = f(\mathbf{x}_i)$. This set of observations forms the dataset from which the surrogate model is initially trained. Following training, and at each iteration of BO, the next location to be expensively evaluated is chosen according to an acquisition function $\alpha(\mathbf{x})$. The location $\mathbf{x}' = \operatorname{argmax}_{\mathbf{x} \in \mathcal{X}} \alpha(\mathbf{x})$ is used as the next location to evaluate. The dataset is augmented with \mathbf{x}' and $f(\mathbf{x}')$ and the process is repeated until the budget is exhausted. The value of the global minimum is then estimated to be the best function evaluation seen during optimisation, i.e. $f^* = \min_i \{f_i\}$.

2.1.1 Gaussian Processes

Gaussian processes (GPs) are commonly used as the surrogate model for f . A GP defines a prior distribution over functions, such that any finite number of function values have a joint Gaussian distribution (Rasmussen and Williams, 2006) with mean $m(\mathbf{x})$ and a covariance $\kappa(\mathbf{x}, \mathbf{x}' | \boldsymbol{\theta})$ with hyperparameters $\boldsymbol{\theta}$. Henceforth, w.l.o.g. we assume a zero-mean

prior $m(\cdot) = 0$. Conditioning the prior distribution on data consisting of f evaluated at t sampled locations $\mathcal{D} = \{(\mathbf{x}_n, f_n \triangleq f(\mathbf{x}_n))\}_{n=1}^t$, the posterior distribution of f is also a GP with posterior mean and variance

$$\mu(\mathbf{x} | \mathcal{D}, \boldsymbol{\theta}) = m(\mathbf{x}) + \boldsymbol{\kappa}(\mathbf{x}, X) K^{-1} \mathbf{f} \quad (1)$$

$$\sigma^2(\mathbf{x} | \mathcal{D}, \boldsymbol{\theta}) = \kappa(\mathbf{x}, \mathbf{x}) - \boldsymbol{\kappa}(\mathbf{x}, X)^\top K^{-1} \boldsymbol{\kappa}(X, \mathbf{x}). \quad (2)$$

Here $X \in \mathbb{R}^{t \times d}$ is the matrix of design locations and $\mathbf{f} = (f_1, f_2, \dots, f_t)^\top$ is the corresponding vector of function evaluations. The kernel matrix $K \in \mathbb{R}^{t \times t}$ is given by $K_{ij} = \kappa(\mathbf{x}_i, \mathbf{x}_j | \boldsymbol{\theta})$ and $\boldsymbol{\kappa}(\mathbf{x}, X) \in \mathbb{R}^t$ is given by $[\boldsymbol{\kappa}(\mathbf{x}, X)]_i = \kappa(\mathbf{x}, \mathbf{x}_i | \boldsymbol{\theta})$. In this work we use an isotropic Matérn 5/2 kernel as recommended for modelling realistic functions (Snoek et al., 2012). The kernel's two hyperparameters $\boldsymbol{\theta}$ are learnt via maximising the log marginal likelihood (Rasmussen and Williams, 2006). Henceforth, we drop the explicit dependencies on \mathcal{D} and $\boldsymbol{\theta}$ for notational simplicity.

2.1.2 Acquisition Functions

The choice of where to evaluate next in BO is determined by an acquisition function $\alpha : \mathbb{R}^d \mapsto \mathbb{R}$. Perhaps the most commonly used acquisition function is Expected Improvement (EI) (Jones et al., 1998), which is defined as the expected positive improvement over the best-seen function value f^* thus far:

$$\alpha_{\text{EI}}(\mathbf{x}) = E_{p(f(\mathbf{x}) | \mathcal{D})} [\max(f^* - f(\mathbf{x}), 0)]. \quad (3)$$

However, many other acquisition functions have also been proposed, including probability of improvement (Kushner, 1964), optimistic strategies such as UCB (Srinivas et al., 2010), ϵ -greedy strategies (De Ath et al., 2020), and information-theoretic approaches (Scott et al., 2011; Hennig and Schuler, 2012; Henrández-Lobato et al., 2014; Wang and Jegelka, 2017; Ru et al., 2018).

2.2 Parallel Bayesian Optimisation

In parallel BO, the algorithm has access to q workers that can evaluate f in parallel and the focus is on minimising the optimisation time, acknowledging that the total computational cost will be greater than for strictly sequential evaluations. The goal is to select a batch of q promising locations to be expensively evaluated in parallel. In the synchronous setting, the BO algorithm sends out a batch of q locations to be evaluated in parallel, and waits for all q evaluations to be completed before submitting the next batch. However, in the asynchronous setting, as soon as a worker has finished evaluating f a new location is submitted to it for evaluation. Therefore, if f takes a variable time to evaluate, the asynchronous version of BO will result in more evaluations of f for the same wallclock time.

One of the earliest synchronous approaches was the qEI method of Ginsbourger et al. (2008), a generalisation of the sequential EI acquisition function (3) that jointly proposes a batch of q locations to evaluate. Similarly, the parallel predictive entropy search (Shah and Ghahramani, 2015) and the parallel knowledge gradient (Wu and Frazier, 2016) also jointly propose q locations and are based on their sequential counterparts. However, these methods require the optimisation of a $d \times q$ problem that becomes prohibitively expensive to solve as q increases (Daxberger and Low, 2017).

Consequently, the prevailing strategy has become to sequentially select the q batch locations. Penalisation-based methods penalise the regions of either the surrogate model (Azimi et al., 2010; Desautels et al., 2014) or the acquisition function that correspond to locations that are currently under evaluation. The Kriging Believer method of Ginsbourger et al. (2010), for example, hallucinates the results of pending evaluations by using the surrogate model's mean prediction as its observed value. The local penalisation methods of Gonzalez et al. (2016) and Alvi et al. (2019) directly penalise an acquisition function. De Ath et al. (2020) show that an ϵ -greedy method that usually exploits the most promising region, with occasional exploratory moves, is effective.

Asynchronous BO has received less attention. Janusevskis et al. (2012) proposed an asynchronous version of the qEI method that uses the qEI criterion assuming that the p locations currently under evaluation are fixed, and optimises the position of the remaining $q - p$ locations. Kandasamy et al. (2018) proposed an approach that uses Thompson Sampling to select locations to evaluate. Thompson sampling (TS) (Thompson, 1933) is a randomised strategy for sequential decision-making under uncertainty (Kandasamy et al., 2018). At each iteration, TS selects the next location to evaluate \mathbf{x}' according to the posterior probability that it is the optimum. If $p_*(\mathbf{x} | \mathcal{D})$ denotes the probability that \mathbf{x} minimises the surrogate model posterior, then

$$p_*(\mathbf{x} | \mathcal{D}) = \int p_*(\mathbf{x} | g) p(g | \mathcal{D}) dg \quad (4)$$

$$= \int \delta(\mathbf{x} - \underset{\mathbf{x} \in \mathcal{X}}{\operatorname{argmin}} g(\mathbf{x})) p(g | \mathcal{D}) dg, \quad (5)$$

where δ is the Dirac delta distribution. Thus, all the probability mass of $p_*(\mathbf{x} | \mathcal{D})$ is at the minimiser of g . In the context of BO, this corresponds to sampling a function $g(\cdot)$ from the surrogate model's posterior $p(\cdot | \mathbf{x}, \mathcal{D})$ and selecting $\mathbf{x}' = \underset{\mathbf{x} \in \mathcal{X}}{\operatorname{argmin}} g(\mathbf{x})$ as the next location to evaluate. This can then be trivially applied in the sequential, synchronous and asynchronous settings by sampling and minimising as many function realisations as required. Thus, the BO loop using TS involves

building a surrogate model with previously evaluated locations (ignoring those that may be currently under evaluation), drawing as many function realisations as there are free workers, finding the minimiser of each realisation and evaluating f at those locations.

Traditionally, g has been approximately optimised by picking the minimum of a randomly sampled set of discrete points (Kandasamy et al., 2018). Recently, Wilson et al. (2020) have identified an elegant decoupled sampling method, which we use here, that decomposes the GP posterior into a sum of a weight-space prior term that is approximated by random Fourier features, and a pathwise update in function space. Unlike other fast approximations, such as (Rahimi and Recht, 2008), this method does not suffer from variance starvation (Calandriello et al., 2019). It scales linearly with the number of locations queried during optimisation of g , and is pathwise differentiable, meaning that gradient-based optimisation can be employed.

Recently, De Palma et al. (2019) proposed a method to draw realisations of acquisition functions instead, by drawing a new set of surrogate model hyperparameters from their priors for each acquisition function. An advantage of these methods is that each draw from either the model posterior or hyperparameter priors defines a new distinct acquisition function. A drawback is that they rely on the uncertainty in the surrogate model to give sufficient diversity in position to the locations selected, unlike acquisition functions which implicitly or explicitly balance exploration and exploitation.

3 AEGiS

It is well recognised that the fundamental problem in global optimisation is to balance exploitation of promising locations found thus far with exploration of new areas which have not been explored. While extremely appealing in its simplicity, Thompson sampling (TS) tends to over-exploit in low dimensions (because after a number of evaluations the posterior variance is reduced and most sampled realisations are similar to the posterior mean), but under-exploit in high dimensions (because there are insufficient samples to drive the posterior variance away from the prior, resulting in effectively random search). The efficacy of ϵ -greedy methods in sequential and synchronous BO over a range of dimensions (De Ath et al., 2020; De Ath et al., 2020) motivates an ϵ -greedy strategy to switch between greedy exploitation of the surrogate model, exploration, and TS. Specifically, at each step we optimise a TS function draw or perform exploration each with probability ϵ , and exploit the surrogate model’s posterior mean prediction $\mu(\mathbf{x})$ of the rest of the time, i.e. with probability $1 - 2\epsilon$.

Algorithm 1 AEGiS

Inputs: \mathcal{D}_t : Training data; T : Evaluation budget.

```

1:  $M = |\mathcal{D}_t|$ 
2: for  $t = M + 1, \dots, T$  do
3:   Condition model posterior on  $\mathcal{D}_t$ ; see (1) and (2)
4:    $r \sim \mathcal{U}(0, 1)$ 
5:   if  $r < 1 - 2\epsilon$  then ▷ Exploit surrogate model
6:      $\mathbf{x}' \leftarrow \underset{\mathbf{x} \in \mathcal{X}}{\operatorname{argmin}} \mu(\mathbf{x})$ 
7:   else if  $r < 1 - \epsilon$  then ▷ Thompson sample
8:      $g \sim p(f | \mathcal{D})$ 
9:      $\mathbf{x}' \leftarrow \underset{\mathbf{x} \in \mathcal{X}}{\operatorname{argmin}} g(\mathbf{x})$ 
10:  else ▷ Approximate Pareto set selection
11:     $\tilde{\mathcal{P}} \leftarrow \text{MOOptimise}_{\mathbf{x} \in \mathcal{X}}(\mu(\mathbf{x}), \sigma^2(\mathbf{x}))$ 
12:     $\mathbf{x}' \leftarrow \text{randomChoice}(\tilde{\mathcal{P}})$ 
13:  Submit new job to evaluate  $\mathbf{x}'$ 
14:  while all workers in use do
15:    Wait for a worker to finish
16:   $\mathcal{D}_t \leftarrow \mathcal{D}_{t-1} \cup \{(\mathbf{x}', f(\mathbf{x}'))\}$  ▷ Augment data

```

The AEGiS method is outlined in Algorithm 1. With probability $1 - 2\epsilon$, the mean prediction from the surrogate model is minimised to find the next location \mathbf{x}' to evaluate (line 6). Alternatively, with probability ϵ , a TS step taken: the next location is determined by sampling a realisation $g(\mathbf{x})$ from the surrogate posterior and finding the minimiser of $g(\mathbf{x})$ (lines 8 and 9). Otherwise (lines 11 and 12), with probability ϵ , the location to evaluate is chosen from the approximate Pareto set of all locations which maximally trade off between exploitation (minimising $\mu(\mathbf{x})$) and exploration (maximising $\sigma^2(\mathbf{x})$). A full discussion is given by De Ath et al. (2020). Briefly, a location \mathbf{x}_1 dominates \mathbf{x}_2 (written $\mathbf{x}_1 \succ \mathbf{x}_2$) iff $\mu(\mathbf{x}_1) \leq \mu(\mathbf{x}_2)$ and $\sigma(\mathbf{x}_1) \geq \sigma(\mathbf{x}_2)$, and at least one of the inequalities is strict. If both $\mathbf{x}_1 \not\succ \mathbf{x}_2$ and $\mathbf{x}_2 \not\succ \mathbf{x}_1$ then \mathbf{x}_1 and \mathbf{x}_2 are said to be mutually non-dominating. The maximal set of mutually non-dominating solutions is known as the Pareto set $\mathcal{P} = \{\mathbf{x} \in \mathcal{X} \mid \mathbf{x}' \not\succ \mathbf{x} \forall \mathbf{x}' \in \mathcal{X}\}$ and comprises the optimal trade-off between exploratory and exploitative locations. Since it is infeasible to enumerate \mathcal{X} , we sample a location from the approximate Pareto set $\tilde{\mathcal{P}} \approx \mathcal{P}$ which is found using a standard multi-objective optimiser (lines 11 and 12).

Selecting a random location from $\tilde{\mathcal{P}}$ ensures that no other location could have been selected that has either more uncertainty given the same predicted value or a lower predicted value given the same amount of uncertainty. Therefore, when considering the two objectives of both reducing the overall model uncertainty and finding the location with the minimum value, these locations are optimal with respect to a specific exploitation-exploration trade-off. Indeed, the maximisers of both EI and UCB are members of \mathcal{P} (De Ath et al., 2020).

Rather than selecting from $\tilde{\mathcal{P}}$, a more exploratory

procedure would be to select from the entire feasible space \mathcal{X} . That is, lines 11 and 12 are replaced with $\mathbf{x}' \leftarrow \text{randomChoice}(\mathcal{X})$. We denote this random selection variant by AEGiS-RS. However, as shown below, it is less effective than selection from $\hat{\mathcal{P}}$.

As discussed above, inaccuracies in the surrogate model provide an element of exploration even when disregarding the uncertainty in the posterior $p(f|\mathcal{D}_t)$. On the other hand, TS tends to be over-exploitative in low dimensions ($d \lesssim 4$) and too exploratory in high dimensions. The performance of sequential ϵ -greedy algorithms is relatively insensitive to the precise choice of ϵ . Here we set $\epsilon = \min(d^{-\frac{1}{2}}, 1/2)$. As shown empirically below, this rate of decay is more effective than faster or slower rates.

4 Experimental Evaluation

We now compare AEGiS with a selection of asynchronous BO methods from the literature. We benchmark them on a selection of well-known synthetic functions in Section 4.1, three meta surrogate benchmarks that mimic the characteristics of hyperparameter tuning problems in Section 4.2 and two robot pushing active learning problems in Section 4.3. Section 4.4 provides an ablation study confirming the importance of each component of AEGiS, experiments on setting ϵ and an evaluation of AEGiS in the sequential setting ($q = 1$ workers).

Methodology and Baselines We compare with four well-known asynchronous BO algorithms: two acquisition function-based penalisation methods, Local Penalisation (LP) (Gonzalez et al., 2016) and the more recent PLAyBOOK (Alvi et al., 2019), as well as the Kriging Believer (KB) (Ginsbourger et al., 2010), all of which are coupled with the expected improvement acquisition function (3). We also include the standard Thompson sampling (TS) approach of Kandasamy et al. (2018) and a purely random approach using Latin hypercube sampling (Random). The Bayesian optimisation pipeline was constructed using GPyTorch (Gardner et al., 2018) and BoTorch (Balandat et al., 2020), and we have made this available online¹.

A zero-mean Gaussian process surrogate model with an isotropic Matérn 5/2 kernel was used in all the experiments. Input variables were rescaled to reside in $[0, 1]^d$ and observations rescaled to have zero-mean and unit variance. The models were initially trained on $M = 2d$ observations generated by maximin Latin hypercube sampling and then optimised for a further 200 – 2d function evaluations. Each optimisation run was re-

Table 1: Benchmark Functions and Dimensionality.

Name	d	Name	d
Branin	2	Ackley	5, 10
Eggholder	2	Michalewicz	5, 10
GoldsteinPrice	2	StyblinskiTang	5, 7, 10
SixHumpCamel	2	Hartmann6	6
Hartmann3	3	Rosenbrock	7, 10

peated 51 times from a different set of Latin hypercube samples. Sets of initial locations were common across all methods to enable statistical comparison. At each iteration, before new locations were selected, the hyperparameters of the GP were optimised by maximising the log likelihood using a multi-restart strategy (Shahriari et al., 2016) with L-BFGS-B (Byrd et al., 1995) and 10 restarts (Algorithm 1, line 3). All experiments were repeated for $q \in \{4, 8, 16\}$ asynchronous workers. We followed the procedure of Kandasamy et al. (2018) to sample an evaluation time for each task, thereby simulating the asynchronous setting. A half-normal distribution was used for this with a scale parameter of $\sqrt{\pi}/2$, giving a mean runtime of 1 (Alvi et al., 2019).

The EI acquisition function in KB, LP and PLAyBOOK, as well as the sampled function from the GP posterior in both TS and AEGiS, and the posterior mean in AEGiS were all optimised using the typical strategy (Balandat et al., 2020) of uniformly sampling 1000d locations in \mathcal{X} , optimising the best 10 of these using L-BFGS-B, and selecting the best as the optimal location. In AEGiS and TS, 2000 Fourier features were used for the decoupled sampling approach of Wilson et al. (2020). The approximate Pareto set $\hat{\mathcal{P}}$ in AEGiS was found using NSGA-II (Deb et al., 2002); see supplementary material.

Here, we report performance in terms of the logarithm of the simple regret R_t , which is the difference between the true minimum value $f(\mathbf{x}^*)$ and the best seen function evaluation up to iteration t : $\log(R_t) = \log(\min\{f_1, \dots, f_t\} - f(\mathbf{x}^*))$.

4.1 Synthetic Experiments

The methods were evaluated on the 15 synthetic benchmark functions listed in Table 1². Figure 1 shows four illustrative convergence plots for the Branin, SixHumpCamel, Ackley, and StyblinskiTang benchmark functions for $q \in \{4, 8, 16\}$ asynchronous workers. Convergence plots and tabulated results for all functions are available in the supplementary material. As can be seen

¹<http://www.github.com/XXXX/XXXX>

²Formulae for all functions can be found at: <http://www.sfu.ca/~ssurjano/optimization.html>.

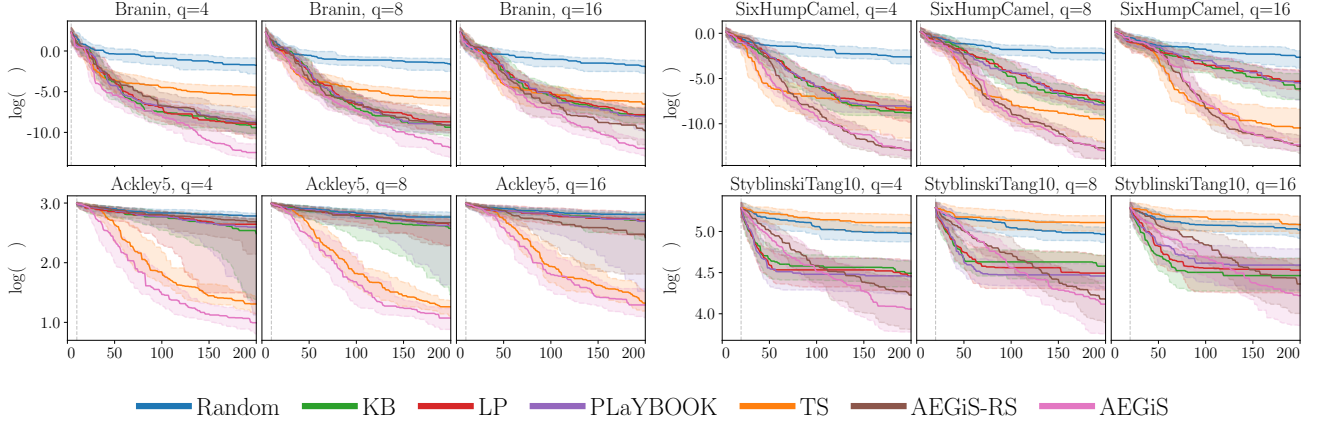


Figure 1: Illustrative convergence plots for four benchmark problems with $q \in \{4, 8, 16\}$ asynchronous workers. Each plot shows the median log simple regret, with shading representing the interquartile range over 51 runs.

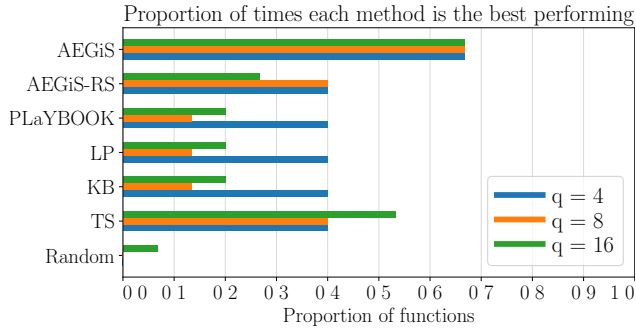


Figure 2: Synthetic function optimisation summary. Bar lengths correspond to the proportion of times that a method is best or statistically equivalent to the best method across the 15 synthetic functions, for $q \in \{4, 8, 16\}$ asynchronous workers.

from the four sets of convergence plots, AEGiS (pink) is almost always better than TS (orange) on all four problems and values of q . Contrastingly, TS is sometimes worse than random search (blue); this is particularly evident on the StyblinskiTang problem. This highlights the effectiveness of both additional exploration and exploitation in AEGiS relative to the TS algorithm. The SixHumpCamel convergence plots show an interesting trend with respect to the penalisation-based methods, namely that they deteriorate at an accelerated rate in comparison to the TS-based methods. We suspect that this is because errors in estimating the correct degree of penalisation accumulate more noticeably as q increases and therefore more function evaluations are placed in unpromising regions.

Figure 2 summarises the performance of each of the evaluated methods for different numbers of workers (q). It shows the number of times each method is the best, i.e. has the lowest median regret over the 51 optimisa-

tion runs, or is statistically indistinguishable from the best method, according to a one-sided, paired Wilcoxon signed-rank test (Knowles et al., 2006) with Holm-Bonferroni correction (Holm, 1979) ($p \geq 0.05$). As is clear from the figure, AEGiS achieves a strong level of performance, and is the best (or equivalent to the best) on 10 out of the 15 functions. AEGiS-RS, which samples exploratory locations from the entire feasible space, is at best equivalent to AEGiS and generally worse. This indicates that using a more informative random sampling scheme, such as selecting from approximate Pareto set of the trade-off between exploitation ($\mu(\mathbf{x})$) and exploration ($\sigma^2(\mathbf{x})$), provides a meaningful improvement to performance.

4.2 Hyperparameter Optimisation

Like Souza et al. (2020), we optimise the hyperparameters of three meta-surrogate optimisation tasks corresponding to a support vector machine (SVM), a fully connected neural network (FC-NET) and the XGBoost algorithm. These problems are part of the Profet benchmark (Klein et al., 2019) and are drawn from generative models built using performance data on multiple datasets. They are designed to mimic the landscape of expensive hyperparameter optimisation tasks, preserving the global landscape characteristics of the modelled methods and giving local variation between function draws from the generative model. This allows for far more evaluations to be carried out than would be possible with the modelled problems. We use Emukit’s implementation (Paley et al., 2019).

Here, we optimise 51 instances of each meta-surrogate, repeating the optimisation $N = 20$ times per instance with different paired training data for each of the N runs. Details of the construction of each problem are given in the supplementary material. The SVM prob-

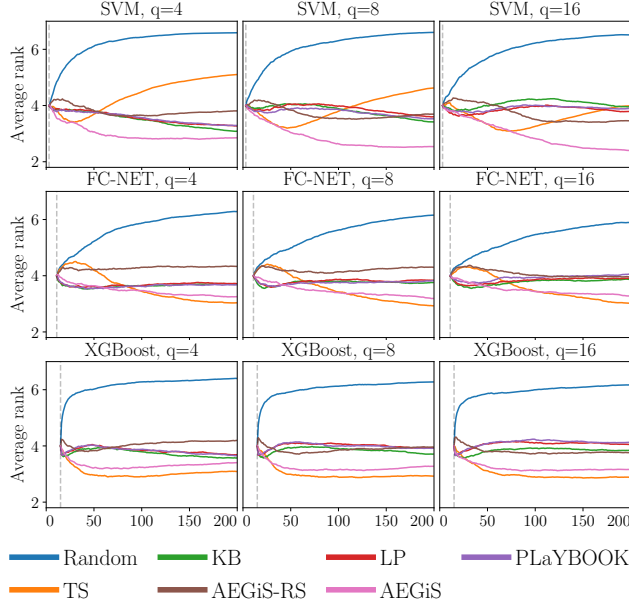


Figure 3: Average ranking scores for the three meta-surrogate benchmarks for $q \in \{4, 8, 16\}$.

lem had 2 parameters; the FC-NET problem 6; and the XGBoost problem 8.

We compare each evaluated method by computing the average ranking score in every iteration for each problem instance. We follow the method of Feurer et al. (2015) and compute this by, for each problem instance, drawing a bootstrap sample of 1000 runs out of the 7^N possible combinations and calculating the fractional ranking after each of the 200 iterations. The ranks are then averaged over all 51 problem instances.

Figure 3 shows the average ranks of the methods on all three problems for $q \in \{4, 8, 16\}$. Similarly to the synthetic functions, all three penalisation methods (KB, LB and PLayBOOK) perform comparably and AEGiS is consistently superior to them after roughly 50 function evaluations. On the FC-NET and XGBoost problems TS performs similarly to AEGiS, and indeed is better on the XGBoost problem. However, AEGiS-RS performs consistently worse supporting the contention that choosing random locations that lie on the Pareto front is generally beneficial and, at worst, does no harm.

4.3 Active Learning for Robot Pushing

Following Wang and Jegelka (2017) and De Ath et al. (2020), we optimise the control parameters for two instance-based active learning robot pushing problems (Wang et al., 2018). In push4, a robot is required to push an object towards an unknown target location. It receives the object-target distance once it has finished pushing. The location of the robot, the orientation of

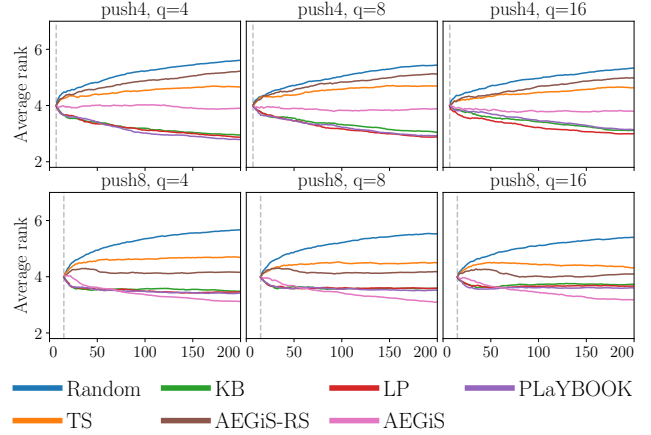


Figure 4: Average ranking scores for the two robot pushing problems for $q \in \{4, 8, 16\}$.

its pushing hand and for how long it pushes are the parameters to be optimised with the goal of minimising this distance. The push8 problem has two robots that receive the distance between their respective objects and targets after pushing — we minimise the sum of these distances. In both problems the target location(s) are chosen randomly, with the constraint that they cannot overlap. We note that the push8 problem is much more difficult because the robots can block each other, and so each problem instance may not be completely solvable. Further details of the problems are provided in the supplementary material.

Average rank score plots, calculated in the same way as described in Section 4.2, are shown in Figure 4. The EI-based methods continue to have very similar performance to one another, and are the best methods on push4, and, even though it is not the best method, AEGiS still out-performs TS consistently. On push8, the EI-based methods initially improve on AEGiS in terms of average rank but then stagnate and are overtaken by AEGiS after roughly 75 function evaluations.

4.4 Additional Experiments

Lastly, we detail an ablation study, experiments on setting the value of ϵ and a comparison between AEGiS, EI and TS in the sequential BO setting ($q = 1$). Full results are available in the supplementary material.

Ablation Study Here, we conduct an ablation study on AEGiS using the 15 synthetic benchmark functions used in Section 4.1. Since AEGiS-RS is consistently outperformed by AEGiS, we omit it from this study. We compare to AEGiS in the following ways: without the exploitation (labelled *No Exploit*); with TS and Pareto set selection having an equal chance of being chosen, no Thompson sampling (*No TS*); with Pareto

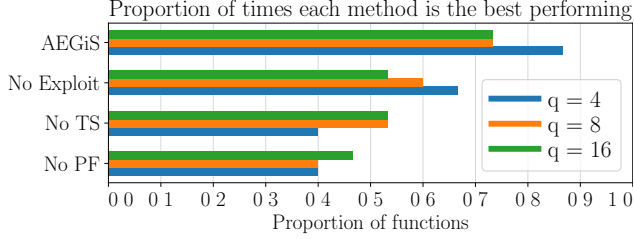


Figure 5: Ablation study summary. The bars correspond to the proportion of times that a method is best or statistically equivalent to the best method across the 15 synthetic functions, for $q \in \{4, 8, 16\}$.

set selection have a probability of 2ϵ of being selected; and no Pareto set selection (*No PF*), with TS having a probability of 2ϵ of being selected.

Figure 5 shows that all three components combine to give the best results and that removing any of the three results in an inferior algorithm. As can be seen, the removal of either TS or Pareto set selection considerably reduces the performance of the algorithm. Note that the results for *No Exploit* are inflated because the method is equivalent to AEGiS on 5 out of the 15 benchmark functions that have $d \leq 4$ dimensions.

Setting ϵ We investigate the rate at which the degree of deliberate exploitation of the surrogate model’s posterior mean function should increase with problem dimensionality d . In AEGiS, exploitation is carried out $1 - 2\epsilon$ proportion of the time, where ϵ was chosen *a priori* to decay like $1/\sqrt{d}$, i.e. $\epsilon = \min(1/\sqrt{d}, 1/2)$. Here, we bracket this decay rate with a quicker decay (more exploitation) and a slower decay (more exploration). Specifically, we evaluate AEGiS on the 15 synthetic test functions using $\epsilon = \min(1/(d-2), 1/2)$ and $\epsilon = \min(1/\log(d+3), 1/2)$ labelled *faster* and *slower* respectively. These values were chosen because they match AEGiS and provide no exploitation when $d \leq 4$, i.e. $\epsilon = 0.5$. Figure 6 summarises the results on the 15 test functions. When using a smaller number of workers, i.e. when $q \in \{4, 8\}$, the $1/\sqrt{d}$ decay gives superior performance. However, when using $q = 16$ there is little to differentiate between the three rates. We note that when d is large the faster rate of the decay is superior (see supplementary material).

Sequential BO Finally, we evaluate AEGiS in the sequential setting, i.e. with $q = 1$. In this setting KB, LP, and PLAyBOOK are equivalent because they all select the next (and only) location to be evaluated using EI. Therefore, we compare AEGiS and AEGiS-RS to TS, EI, and Latin hypercube sampling. As shown in the supplementary material, AEGiS and EI had approximately equivalent performance, and they

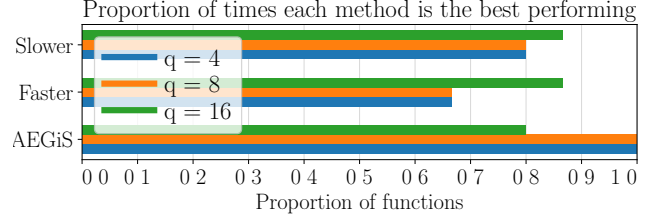


Figure 6: Selecting ϵ : *faster* and *slower* correspond to quicker and slower rates of ϵ decay than AEGiS, resulting in more or less exploitation respectively.

were both superior to AEGiS-RS and TS. This again highlights the importance of sampling from $\tilde{\mathcal{P}}$. An ablation study was also carried with similar findings: removing the sampling from $\tilde{\mathcal{P}}$ led to a large reduction in performance. This was a larger drop in performance in comparison to the ablation study using larger values of q . We suspect that this is because the model will naturally be of a higher quality at any iteration for $q = 1$ and thus selection from $\tilde{\mathcal{P}}$ will be even more informative to the optimisation process. Different rates of ϵ decay were also investigated as before, and similar results were found: both decreasing and increasing the rate of decay led to worse performance, with the largest decrease coming from increasing the rate and thus increasing exploitation further.

5 Conclusion

Recent work has shown that ϵ -greedy methods which usually exploit the surrogate mean prediction together with occasional deliberate exploratory moves are effective, because modelling inaccuracies provide inadvertent exploration. AEGiS, which combines greedy exploitation with Thompson sampling and exploratory moves from the approximate Pareto set that maximally trades off exploration and exploitation, generally outperforms existing asynchronous BO methods. The ablation study verifies the importance of each of the three components of AEGiS and shows that selection of exploratory locations from the approximate Pareto set is superior to random selection from the feasible space. With only a single worker this simple algorithm is no worse than BO using expected improvement.

Future work will involve bounding the regret of AEGiS, building upon the bounds for TS (Kandasamy et al., 2018), and modelling the likelihood that an unfinished job should be stopped early because it will not provide useful information.

Acknowledgments

This work was supported by Innovate UK grant 104400.

References

- Alvi, A., Ru, B., Calliess, J.-P., Roberts, S., and Osborne, M. A. (2019). Asynchronous batch Bayesian optimisation with improved local penalisation. In *International Conference on Machine Learning*, pages 253–262.
- Azimi, J., Fern, A., and Fern, X. Z. (2010). Batch Bayesian optimization via simulation matching. In *Advances in Neural Information Processing Systems*, pages 109–117. Curran Associates, Inc.
- Balandat, M., Karrer, B., Jiang, D. R., Daulton, S., Letham, B., Wilson, A. G., and Bakshy, E. (2020). BoTorch: Programmable Bayesian optimization in PyTorch. *arXiv preprint arXiv:1910.06403*.
- Brochu, E., Cora, V. M., and de Freitas, N. (2010). A tutorial on Bayesian optimization of expensive cost functions, with application to active user modeling and hierarchical reinforcement learning. *arXiv preprint arXiv:1012.2599*.
- Byrd, R. H., Lu, P., Nocedal, J., and Zhu, C. (1995). A limited memory algorithm for bound constrained optimization. *SIAM Journal on Scientific Computing*, 16(5):1190–1208.
- Calandriello, D., Carratino, L., Lazaric, A., Valko, M., and Rosasco, L. (2019). Gaussian process optimization with adaptive sketching: Scalable and no regret. In *Conference on Learning Theory*, pages 533–557. PMLR.
- Chen, Y., Huang, A., Wang, Z., Antonoglou, I., Schrittwieser, J., Silver, D., and de Freitas, N. (2018). Bayesian optimization in AlphaGo. *arXiv preprint arXiv:1812.06855*.
- Daxberger, E. A. and Low, B. K. H. (2017). Distributed batch Gaussian process optimization. In *International Conference on Machine Learning*, pages 951–960. PMLR.
- De Ath, G., Everson, R. M., Fieldsend, J. E., and Rahat, A. A. M. (2020). ϵ -shotgun: ϵ -greedy batch Bayesian optimisation. In *Proceedings of the 2020 Genetic and Evolutionary Computation Conference*, pages 787–795. Association for Computing Machinery.
- De Ath, G., Everson, R. M., Rahat, A. A. M., and Fieldsend, J. E. (2020). Greed is good: Exploration and exploitation trade-offs in Bayesian optimisation. *arXiv preprint arXiv:1911.12809*.
- De Palma, A., Mendler-Dünner, C., Parnell, T., Anghel, A., and Pozidis, H. (2019). Sampling acquisition functions for batch Bayesian optimization. *arXiv preprint arXiv:1903.09434*.
- Deb, K., Pratap, A., Agarwal, S., and Meyarivan, T. (2002). A fast and elitist multiobjective genetic algorithm: NSGA-II. *IEEE Transactions on Evolutionary Computation*, 6(2):182–197.
- Desautels, T., Krause, A., and Burdick, J. W. (2014). Parallelizing exploration-exploitation tradeoffs in Gaussian process bandit optimization. *Journal of Machine Learning Research*, 15(119):4053–4103.
- Feurer, M., Springenberg, J. T., and Hutter, F. (2015). Initializing Bayesian hyperparameter optimization via meta-learning. In *Proceedings of the Twenty-Ninth AAAI Conference on Artificial Intelligence*, pages 1128–1135. AAAI Press.
- Gardner, J., Pleiss, G., Weinberger, K. Q., Bindel, D., and Wilson, A. G. (2018). GPyTorch: Blackbox matrix-matrix Gaussian process inference with GPU acceleration. In *Advances in Neural Information Processing Systems 31*, pages 7576–7586. Curran Associates, Inc.
- Ginsbourger, D., Le Riche, R., and Carraro, L. (2008). A multi-points criterion for deterministic parallel global optimization based on Gaussian processes. <https://hal.archives-ouvertes.fr/hal-00260579>.
- Ginsbourger, D., Le Riche, R., and Carraro, L. (2010). Kriging is well-suited to parallelize optimization. In *Computational Intelligence in Expensive Optimization Problems*, volume 2, pages 131–162. Springer.
- Gonzalez, J., Dai, Z., Hennig, P., and Lawrence, N. (2016). Batch Bayesian optimization via local penalization. In *Artificial Intelligence and Statistics*, pages 648–657.
- Gupta, S., Shilton, A., Rana, S., and Venkatesh, S. (2018). Exploiting strategy-space diversity for batch Bayesian optimization. In *International Conference on Artificial Intelligence and Statistics*, pages 538–547.
- Hennig, P. and Schuler, C. J. (2012). Entropy search for information-efficient global optimization. *Journal of Machine Learning Research*, 13(1):1809–1837.
- Henrández-Lobato, J. M., Hoffman, M. W., and Ghahramani, Z. (2014). Predictive entropy search for efficient global optimization of black-box functions. In *Proceedings of the 27th International Conference on Neural Information Processing Systems*, pages 918–926. MIT Press.
- Hernández-Lobato, J. M., Requeima, J., Pyzer-Knapp, E. O., and Aspuru-Guzik, A. (2017). Parallel and distributed Thompson sampling for large-scale accelerated exploration of chemical space. In *Proceedings of the 34th International Conference on Machine Learning*, pages 1470–1479. PMLR.
- Holm, S. (1979). A simple sequentially rejective multiple test procedure. *Scandinavian Journal of Statistics*, 6(2):65–70.

- Janusevskis, J., Le Riche, R., Ginsbourger, D., and Girdziusas, R. (2012). Expected improvements for the asynchronous parallel global optimization of expensive functions. In *Learning and Intelligent Optimization*, volume 7219, pages 413–418. Springer.
- Jones, D. R., Schonlau, M., and Welch, W. J. (1998). Efficient global optimization of expensive black-box functions. *Journal of Global Optimization*, 13(4):455–492.
- Kandasamy, K., Krishnamurthy, A., Schneider, J., and Póczos, B. (2018). Parallelised Bayesian optimisation via Thompson sampling. In *International Conference on Artificial Intelligence and Statistics*, pages 133–142.
- Klein, A., Dai, Z., Hutter, F., Lawrence, N., and Gonzalez, J. (2019). Meta-surrogate benchmarking for hyperparameter optimization. In *Advances in Neural Information Processing Systems 32*, pages 6270–6280. Curran Associates, Inc.
- Knowles, J. D., Thiele, L., and Zitzler, E. (2006). A tutorial on the performance assesment of stochastic multiobjective optimizers. Technical Report TIK214, Computer Engineering and Networks Laboratory, ETH Zurich, Zurich, Switzerland.
- Kushner, H. J. (1964). A new method of locating the maximum point of an arbitrary multipeak curve in the presence of noise. *Journal Basic Engineering*, 86(1):97–106.
- McKay, M. D., Beckman, R. J., and Conover, W. J. (1979). A comparison of three methods for selecting values of input variables in the analysis of output from a computer code. *Technometrics*, 21(2):239–245.
- Paleyes, A., Pullin, M., Mahsereci, M., Lawrence, N., and González, J. (2019). Emulation of physical processes with Emukit. In *Second Workshop on Machine Learning and the Physical Sciences, NeurIPS*.
- Rahimi, A. and Recht, B. (2008). Random features for large-scale kernel machines. In *Advances in Neural Information Processing Systems 20*, pages 1177–1184. Curran Associates, Inc.
- Rasmussen, C. E. and Williams, C. K. I. (2006). *Gaussian processes for machine learning*. The MIT Press, Boston, MA.
- Ru, B., Osborne, M. A., Mcleod, M., and Granzol, D. (2018). Fast information-theoretic Bayesian optimisation. In *Proceedings of the 35th International Conference on Machine Learning*, pages 4384–4392. PMLR.
- Scott, W., Frazier, P., and Powell, W. (2011). The correlated knowledge gradient for simulation optimization of continuous parameters using Gaussian process regression. *SIAM Journal on Optimization*, 21(3):996–1026.
- Shah, A. and Ghahramani, Z. (2015). Parallel predictive entropy search for batch global optimization of expensive objective functions. In *Advances in Neural Information Processing Systems*, pages 3330–3338. Curran Associates, Inc.
- Shahriari, B., Swersky, K., Wang, Z., Adams, R. P., and de Freitas, N. (2016). Taking the human out of the loop: A review of Bayesian optimization. *Proceedings of the IEEE*, 104(1):148–175.
- Snoek, J., Larochelle, H., and Adams, R. P. (2012). Practical Bayesian optimization of machine learning algorithms. In *Advances in Neural Information Processing Systems*, pages 2951–2959. Curran Associates, Inc.
- Souza, A., Nardi, L., Oliveira, L. B., Olukotun, K., Lindauer, M., and Hutter, F. (2020). Prior-guided Bayesian optimization. *arXiv preprint arXiv:2006.14608*.
- Srinivas, N., Krause, A., Kakade, S., and Seeger, M. (2010). Gaussian process optimization in the bandit setting: No regret and experimental design. In *Proceedings of the 27th International Conference on Machine Learning*, pages 1015–1022. Omnipress.
- Thompson, W. R. (1933). On the likelihood that one unknown probability exceeds another in view of the evidence of two samples. *Biometrika*, 25(3/4):285–294.
- Wang, Z., Garrett, C. R., Kaelbling, L. P., and Lozano-Perez, T. (2018). Active model learning and diverse action sampling for task and motion planning. In *International Conference on Intelligent Robots and Systems (IROS)*.
- Wang, Z. and Jegelka, S. (2017). Max-value entropy search for efficient Bayesian optimization. In *Proceedings of the 34th International Conference on Machine Learning*, pages 3627–3635. PMLR.
- Wilson, J., Borovitskiy, V., Terenin, A., Mostowsky, P., and Deisenroth, M. (2020). Efficiently sampling functions from Gaussian process posteriors. In *Proceedings of the 37th International Conference on Machine Learning*. PMLR.
- Wu, J. and Frazier, P. (2016). The parallel knowledge gradient method for batch Bayesian optimization. In *Advances in Neural Information Processing Systems*, pages 3126–3134. Curran Associates, Inc.

Asynchronous ϵ -Greedy Bayesian Optimisation: Supplementary Materials

1 Experimental details

Here we give additional details of the algorithms used.

NSGA-II To find the approximate Pareto set we used NSGA-II (Deb et al., 2002) with a population size of $100d$, a mutation rate of d^{-1} , a crossover rate of 0.8, and mutation and distribution indices of $\eta_c = \eta_m = 20$.

2 Additional Results: Synthetic Functions

In this section we show all convergence plots and results tables for the synthetic function experiments. Figures 1, 2, 3, and 4 show the convergence plots for each of the six methods on the fifteen benchmark problems for $q \in \{4, 8, 16\}$. Each plot shows the median log simple regret, with shading representing the interquartile range over 51 runs. Tables 1, 2 and 3 show the median log simple regret as well as the median absolute deviation from the median (MAD), a robust measure of dispersion. The method with the best (lowest) median regret is shown in dark grey, and those that are statistically equivalent to the best method according to a one-sided, paired Wilcoxon signed-rank test with Holm-Bonferroni correction (Holm, 1979) ($p \geq 0.05$) are shown in light grey.

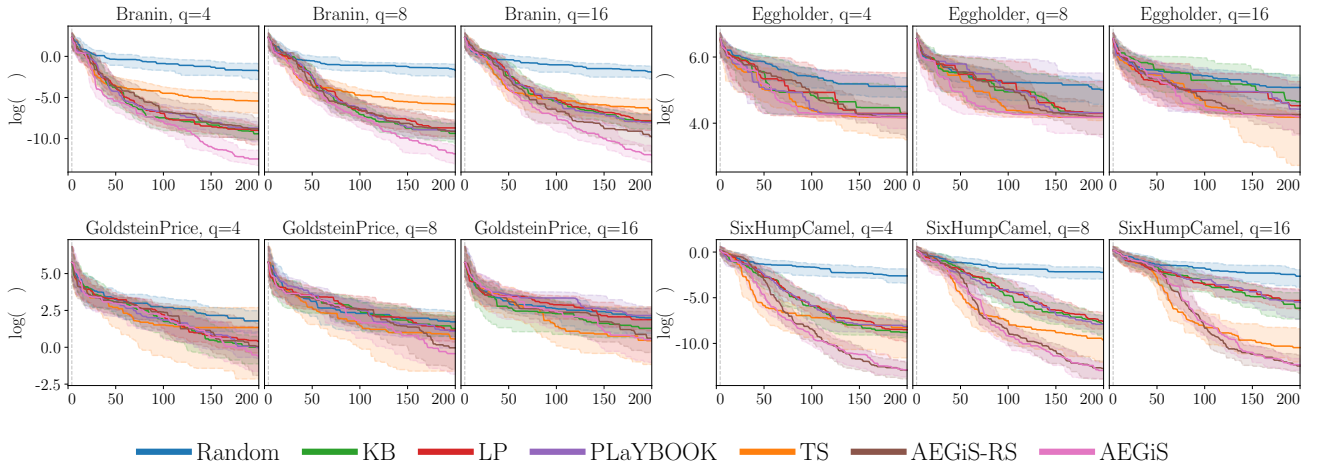


Figure 1: Convergence results for the synthetic test problems.

Table 1: Tabulated results for $q = 4$ asynchronous workers, showing the median log simple regret (*left*) and median absolute deviation from the median (MAD, *right*) after 200 function evaluations across the 51 runs. The method with the lowest median performance is shown in dark grey, with those with statistically equivalent performance are shown in light grey.

Method	Branin (2)		Eggholder (2)		GoldsteinPrice (2)		SixHumpCamel (2)		Hartmann3 (3)	
	Median	MAD	Median	MAD	Median	MAD	Median	MAD	Median	MAD
Random	1.73×10^{-1}	2.02×10^{-1}	1.66×10^2	7.34×10^1	5.99	6.22	7.35×10^{-2}	6.39×10^{-2}	1.71×10^{-1}	1.07×10^{-1}
TS	4.39×10^{-3}	5.65×10^{-3}	6.51×10^1	2.06×10^1	3.81	5.60	2.60×10^{-4}	3.84×10^{-4}	1.08×10^{-2}	1.57×10^{-2}
KB	8.14×10^{-5}	1.16×10^{-4}	7.20×10^1	9.85×10^1	1.01	1.13	1.48×10^{-4}	1.43×10^{-4}	1.09×10^{-4}	1.29×10^{-4}
LP	1.24×10^{-4}	1.54×10^{-4}	7.32×10^1	9.70×10^1	1.49	1.42	2.05×10^{-4}	2.62×10^{-4}	1.06×10^{-4}	1.42×10^{-4}
PLaYBOOK	1.58×10^{-4}	1.96×10^{-4}	7.11×10^1	1.31×10^1	9.61×10^{-1}	1.04	2.92×10^{-4}	2.97×10^{-4}	1.25×10^{-4}	1.50×10^{-4}
AEgIS-RS	1.39×10^{-4}	1.96×10^{-4}	6.51×10^1	2.78×10^1	1.05	1.48	2.39×10^{-6}	2.79×10^{-6}	1.28×10^{-2}	1.61×10^{-2}
AEgIS	3.82×10^{-6}	4.67×10^{-6}	6.51×10^1	8.35	5.09×10^{-1}	6.15×10^{-1}	2.53×10^{-6}	2.82×10^{-6}	6.73×10^{-5}	8.80×10^{-5}

Method	Ackley5 (5)		Michalewicz5 (5)		StyblinskiTang5 (5)		Hartmann6 (6)		Rosenbrock7 (7)	
	Median	MAD	Median	MAD	Median	MAD	Median	MAD	Median	MAD
Random	1.62×10^1	1.71	2.19	2.81×10^{-1}	4.50×10^1	1.00×10^1	9.57×10^{-1}	3.60×10^{-1}	1.31×10^4	9.64×10^3
TS	3.70	8.13×10^{-1}	2.06	5.05×10^{-1}	1.45×10^1	2.05×10^1	2.78×10^{-3}	3.25×10^{-3}	3.00×10^2	2.54×10^2
KB	1.21×10^1	5.72	1.03	8.01×10^{-1}	1.46×10^1	4.55	7.51×10^{-3}	1.04×10^{-2}	5.42×10^2	3.00×10^2
LP	1.41×10^1	4.13	1.02	5.61×10^{-1}	1.47×10^1	5.64	4.34×10^{-3}	5.40×10^{-3}	5.86×10^2	3.31×10^2
PLaYBOOK	1.34×10^1	4.81	1.13	6.83×10^{-1}	1.46×10^1	1.24×10^1	4.32×10^{-3}	5.37×10^{-3}	4.45×10^2	3.00×10^2
AEgIS-RS	1.47×10^1	3.95	2.17	3.35×10^{-1}	1.45×10^1	1.21×10^1	7.62×10^{-3}	1.03×10^{-2}	5.37×10^2	3.14×10^2
AEgIS	2.70	6.70×10^{-1}	1.48	5.05×10^{-1}	1.47×10^1	6.34	3.76×10^{-3}	5.26×10^{-3}	4.47×10^2	3.45×10^2

Method	StyblinskiTang7 (7)		Ackley10 (10)		Michalewicz10 (10)		Rosenbrock10 (10)		StyblinskiTang10 (10)	
	Median	MAD	Median	MAD	Median	MAD	Median	MAD	Median	MAD
Random	8.18×10^1	1.32×10^1	1.93×10^1	5.27×10^{-1}	9.98×10^{-1}	4.53×10^{-1}	5.91×10^4	3.31×10^4	1.44×10^2	1.87×10^1
TS	8.14×10^1	3.55×10^1	1.10×10^1	1.97	1.24	4.07×10^{-1}	6.34×10^2	4.05×10^2	1.65×10^2	2.55×10^1
KB	4.27×10^1	1.29×10^1	1.67×10^1	1.55	2.68×10^{-1}	3.55×10^{-1}	1.53×10^3	9.03×10^2	8.93×10^1	2.13×10^1
LP	4.54×10^1	1.61×10^1	1.59×10^1	2.48	2.23×10^{-1}	3.04×10^{-1}	1.45×10^3	8.25×10^2	8.62×10^1	2.74×10^1
PLaYBOOK	4.20×10^1	1.29×10^1	1.62×10^1	2.26	1.83×10^{-1}	2.50×10^{-1}	1.46×10^3	9.33×10^2	8.58×10^1	2.71×10^1
AEgIS-RS	3.22×10^1	1.60×10^1	1.84×10^1	7.77×10^{-1}	8.52×10^{-1}	6.00×10^{-1}	8.69×10^2	5.11×10^2	6.85×10^1	2.54×10^1
AEgIS	3.21×10^1	1.61×10^1	1.34×10^1	2.80	5.87×10^{-1}	5.78×10^{-1}	9.45×10^2	7.03×10^2	5.78×10^1	3.10×10^1

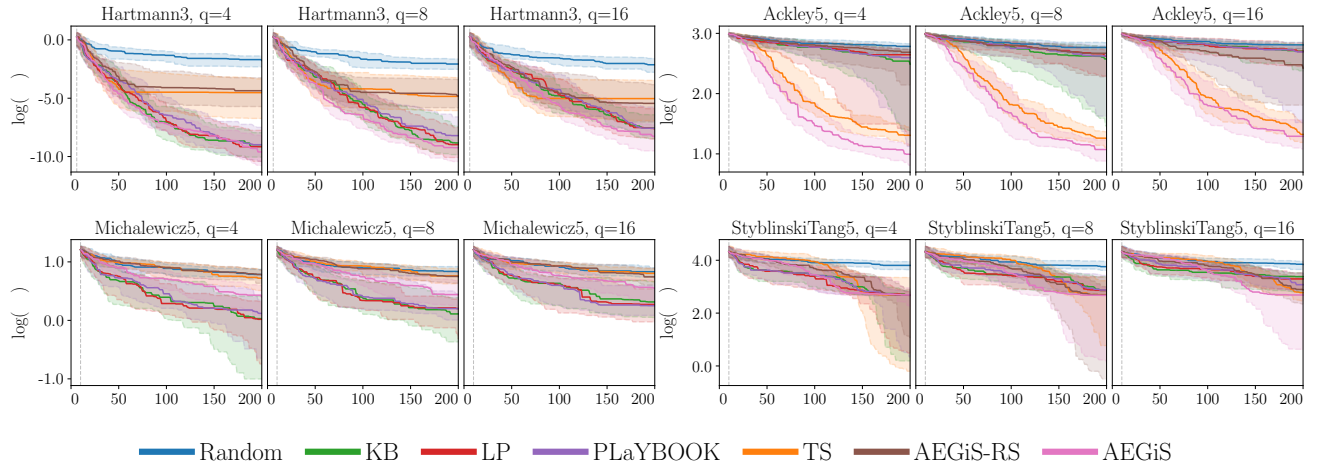


Figure 2: Convergence results for the synthetic test problems.

Table 2: Tabulated results for $q = 8$ asynchronous workers, showing the median log simple regret (*left*) and median absolute deviation from the median (MAD, *right*) after 200 function evaluations across the 51 runs. The method with the lowest median performance is shown in dark grey, with those with statistically equivalent performance are shown in light grey.

Method	Brannin (2)		Eggholder (2)		GoldsteinPrice (2)		SixHumpCamel (2)		Hartmann3 (3)	
	Median	MAD	Median	MAD	Median	MAD	Median	MAD	Median	MAD
Random	1.81×10^{-1}	2.21×10^{-1}	1.50×10^2	7.39×10^1	5.61	6.48	1.09×10^{-1}	8.72×10^{-2}	1.26×10^{-1}	8.14×10^{-2}
TS	2.91×10^{-3}	3.73×10^{-3}	6.51×10^1	9.41	1.76	2.60	6.73×10^{-5}	9.86×10^{-5}	7.89×10^{-3}	1.07×10^{-2}
KB	8.55×10^{-5}	1.14×10^{-4}	7.39×10^1	6.63×10^1	3.57	3.41	3.75×10^{-4}	4.68×10^{-4}	1.46×10^{-4}	1.69×10^{-4}
LP	1.66×10^{-4}	1.76×10^{-4}	7.37×10^1	8.40×10^1	3.18	3.19	5.13×10^{-4}	5.47×10^{-4}	1.26×10^{-4}	1.59×10^{-4}
PLaYBOOK	1.10×10^{-4}	1.27×10^{-4}	7.48×10^1	7.94×10^1	2.97	3.67	3.66×10^{-4}	4.38×10^{-4}	2.73×10^{-4}	3.28×10^{-4}
AEgIS-RS	1.09×10^{-4}	1.19×10^{-4}	6.64×10^1	4.31×10^1	9.66×10^{-1}	1.39	2.92×10^{-6}	3.27×10^{-6}	8.17×10^{-3}	1.16×10^{-2}
AEgIS	7.10×10^{-6}	8.66×10^{-6}	6.51×10^1	2.76×10^1	6.48×10^{-1}	8.22×10^{-1}	2.35×10^{-6}	2.83×10^{-6}	9.71×10^{-5}	9.88×10^{-5}

Method	Ackley5 (5)		Michalewicz5 (5)		StyblinskiTang5 (5)		Hartmann6 (6)		Rosenbrock7 (7)	
	Median	MAD	Median	MAD	Median	MAD	Median	MAD	Median	MAD
Random	1.59×10^1	2.07	2.30	2.86×10^{-1}	4.29×10^1	1.22×10^1	1.05	3.09×10^{-1}	1.33×10^4	7.34×10^3
TS	3.53	6.96×10^{-1}	2.14	4.66×10^{-1}	1.48×10^1	1.68×10^1	4.17×10^{-3}	4.99×10^{-3}	3.42×10^2	2.79×10^2
KB	1.31×10^1	5.66	1.12	6.19×10^{-1}	1.74×10^1	1.68×10^1	1.01×10^{-2}	1.37×10^{-2}	8.14×10^2	4.87×10^2
LP	1.37×10^1	3.02	1.23	4.53×10^{-1}	1.74×10^1	1.20×10^1	6.42×10^{-3}	8.18×10^{-3}	9.32×10^2	5.76×10^2
PLaYBOOK	1.38×10^1	4.38	1.22	4.05×10^{-1}	1.77×10^1	1.73×10^1	1.25×10^{-2}	1.78×10^{-2}	7.10×10^2	4.25×10^2
AEgIS-RS	1.44×10^1	3.48	2.11	2.98×10^{-1}	1.46×10^1	1.98×10^1	7.11×10^{-3}	8.85×10^{-3}	8.65×10^2	5.77×10^2
AEgIS	2.92	7.50×10^{-1}	1.55	5.89×10^{-1}	1.44×10^1	1.79×10^1	2.23×10^{-3}	2.71×10^{-3}	6.19×10^2	5.82×10^2

Method	StyblinskiTang7 (7)		Ackley10 (10)		Michalewicz10 (10)		Rosenbrock10 (10)		StyblinskiTang10 (10)	
	Median	MAD	Median	MAD	Median	MAD	Median	MAD	Median	MAD
Random	8.26×10^1	1.67×10^1	1.93×10^1	3.95×10^{-1}	1.16	4.68×10^{-1}	5.88×10^4	2.73×10^4	1.43×10^2	1.82×10^1
TS	8.65×10^1	2.52×10^1	1.01×10^1	2.46	1.04	4.71×10^{-1}	6.52×10^2	4.64×10^2	1.65×10^2	2.38×10^1
KB	4.96×10^1	1.70×10^1	1.66×10^1	1.28	2.41×10^{-1}	3.17×10^{-1}	2.40×10^3	1.65×10^3	9.73×10^1	2.26×10^1
LP	4.83×10^1	1.88×10^1	1.62×10^1	1.75	2.49×10^{-1}	3.24×10^{-1}	2.16×10^3	1.14×10^3	8.94×10^1	2.89×10^1
PLaYBOOK	5.27×10^1	2.19×10^1	1.60×10^1	1.66	3.13×10^{-1}	4.01×10^{-1}	2.14×10^3	1.30×10^3	8.64×10^1	1.95×10^1
AEgIS-RS	4.25×10^1	1.91×10^1	1.82×10^1	1.38	9.71×10^{-1}	4.83×10^{-1}	1.09×10^3	8.64×10^2	6.50×10^1	2.25×10^1
AEgIS	4.27×10^1	1.98×10^1	1.37×10^1	2.93	6.68×10^{-1}	6.68×10^{-1}	1.26×10^3	7.68×10^2	6.14×10^1	2.79×10^1

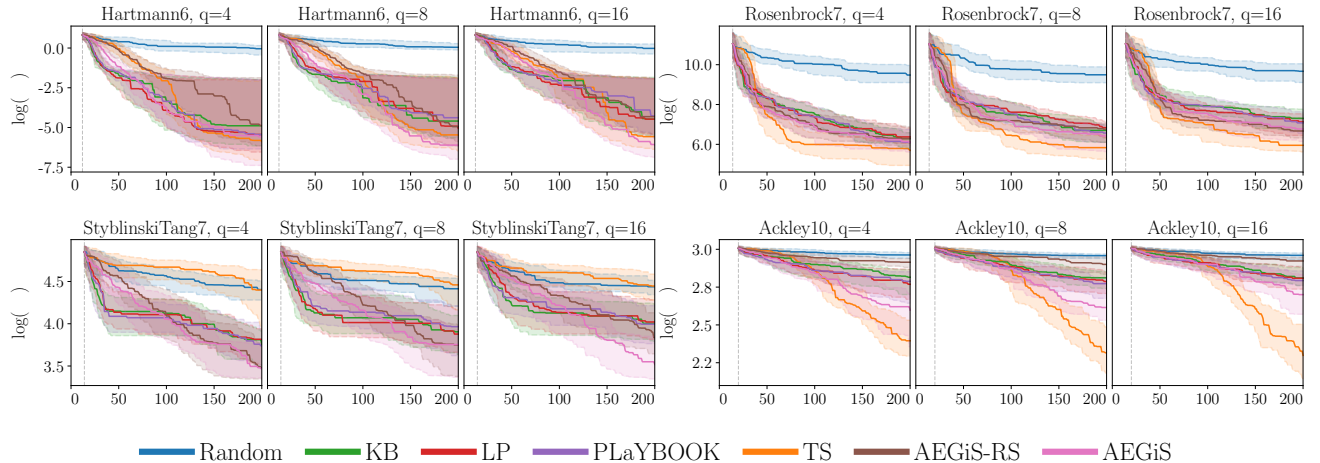


Figure 3: Convergence results for the synthetic test problems.

Table 3: Tabulated results for $q = 16$ asynchronous workers, showing the median log simple regret (*left*) and median absolute deviation from the median (MAD, *right*) after 200 function evaluations across the 51 runs. The method with the lowest median performance is shown in dark grey, with those with statistically equivalent performance are shown in light grey.

Method	Brannin (2)		Eggholder (2)		GoldsteinPrice (2)		SixHumpCamel (2)		Hartmann3 (3)	
	Median	MAD	Median	MAD	Median	MAD	Median	MAD	Median	MAD
Random	1.45×10^{-1}	1.47×10^{-1}	1.61×10^2	1.05×10^2	7.34	8.20	7.09×10^{-2}	7.83×10^{-2}	1.19×10^{-1}	1.01×10^{-1}
TS	1.47×10^{-3}	2.11×10^{-3}	6.51×10^1	4.59×10^1	1.56	2.29	2.86×10^{-5}	3.62×10^{-5}	6.53×10^{-3}	9.08×10^{-3}
KB	3.53×10^{-4}	3.72×10^{-4}	1.04×10^2	8.39×10^1	3.62	3.45	2.14×10^{-3}	3.07×10^{-3}	5.25×10^{-4}	6.34×10^{-4}
LP	3.99×10^{-4}	4.98×10^{-4}	9.27×10^1	8.75×10^1	6.52	6.35	4.97×10^{-3}	6.41×10^{-3}	4.96×10^{-4}	6.01×10^{-4}
PLaYBOOK	3.18×10^{-4}	4.11×10^{-4}	8.36×10^1	8.29×10^1	8.66	9.65	4.02×10^{-3}	5.46×10^{-3}	5.15×10^{-4}	6.17×10^{-4}
AEGIS-RS	5.47×10^{-5}	7.30×10^{-5}	7.07×10^1	2.74×10^1	1.77	2.32	3.85×10^{-6}	4.28×10^{-6}	4.33×10^{-3}	6.27×10^{-3}
AEGIS	5.88×10^{-6}	8.01×10^{-6}	6.54×10^1	1.49×10^1	1.67	2.27	4.40×10^{-6}	4.38×10^{-6}	2.53×10^{-4}	3.04×10^{-4}

Method	Ackley5 (5)		Michalewicz5 (5)		StyblinskiTang5 (5)		Hartmann6 (6)		Rosenbrock7 (7)	
	Median	MAD	Median	MAD	Median	MAD	Median	MAD	Median	MAD
Random	1.66×10^1	1.22	2.30	3.03×10^{-1}	4.67×10^1	9.10	9.78×10^{-1}	4.73×10^{-1}	1.58×10^4	1.03×10^4
TS	3.75	7.74×10^{-1}	2.23	3.20×10^{-1}	1.60×10^1	1.29×10^1	3.79×10^{-3}	4.91×10^{-3}	3.84×10^2	2.63×10^2
KB	1.49×10^1	3.57	1.37	6.89×10^{-1}	2.93×10^1	1.65×10^1	1.14×10^{-2}	1.53×10^{-2}	1.49×10^3	1.18×10^3
LP	1.49×10^1	4.20	1.31	5.50×10^{-1}	2.69×10^1	1.25×10^1	1.14×10^{-2}	1.48×10^{-2}	1.25×10^3	9.30×10^2
PLaYBOOK	1.48×10^1	3.31	1.29	5.21×10^{-1}	2.17×10^1	1.43×10^1	1.40×10^{-2}	1.93×10^{-2}	1.18×10^3	8.95×10^2
AEGIS-RS	1.13×10^1	6.40	2.10	4.70×10^{-1}	1.78×10^1	1.42×10^1	1.33×10^{-2}	1.70×10^{-2}	7.87×10^2	5.00×10^2
AEGIS	3.64	1.30	1.73	4.50×10^{-1}	1.47×10^1	1.86×10^1	2.25×10^{-3}	2.70×10^{-3}	8.72×10^2	6.23×10^2

Method	StyblinskiTang7 (7)		Ackley10 (10)		Michalewicz10 (10)		Rosenbrock10 (10)		StyblinskiTang10 (10)	
	Median	MAD	Median	MAD	Median	MAD	Median	MAD	Median	MAD
Random	8.46×10^1	1.09×10^1	1.93×10^1	5.99×10^{-1}	1.14	3.89×10^{-1}	5.93×10^4	2.66×10^4	1.51×10^2	1.79×10^1
TS	8.53×10^1	2.04×10^1	9.96	2.36	1.18	4.44×10^{-1}	6.55×10^2	3.56×10^2	1.61×10^2	2.42×10^1
KB	5.48×10^1	1.99×10^1	1.66×10^1	1.54	4.65×10^{-1}	4.75×10^{-1}	2.87×10^3	1.44×10^3	8.68×10^1	2.69×10^1
LP	5.58×10^1	1.96×10^1	1.66×10^1	1.90	4.01×10^{-1}	5.35×10^{-1}	3.13×10^3	1.86×10^3	9.27×10^1	2.58×10^1
PLaYBOOK	5.43×10^1	1.69×10^1	1.63×10^1	8.28×10^{-1}	2.83×10^{-1}	3.45×10^{-1}	3.23×10^3	2.04×10^3	9.86×10^1	3.53×10^1
AEGIS-RS	4.63×10^1	1.70×10^1	1.86×10^1	6.95×10^{-1}	1.04	5.74×10^{-1}	1.56×10^3	6.77×10^2	7.84×10^1	3.30×10^1
AEGIS	3.37×10^1	1.93×10^1	1.49×10^1	2.99	7.84×10^{-1}	5.67×10^{-1}	1.77×10^3	1.13×10^3	6.81×10^1	3.26×10^1

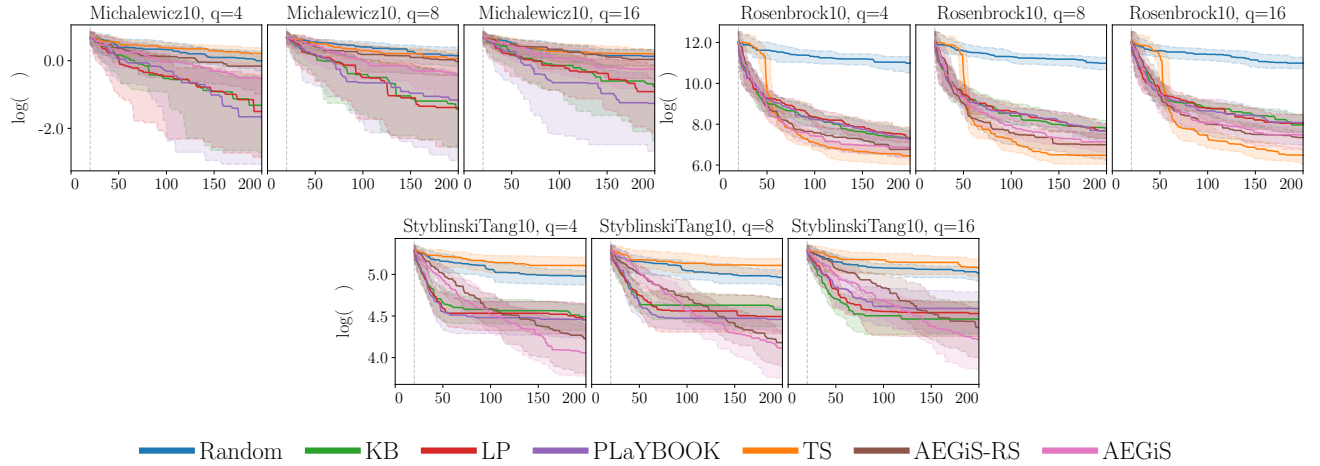


Figure 4: Convergence results for the synthetic test problems.

3 Instance-based Problems

In this section we give further details of the hyperparameter optimisation benchmark problems and the robot pushing problems, as well as providing the average rank score plots for each problem.

3.1 Hyperparameter Optimisation Benchmark

The SVM problem was built using a set of SVM classification models trained on 16 OpenML tasks, with 2 input parameters corresponding to the SVM’s hyperparameters. The FC-NET problem was built using a set of feed-forward neural networks trained on the same OpenML tasks, with 6 input parameters corresponding to the network hyperparameters. XGBoost was built using a set of XGBoost regression models trained on 11 UCI datasets and has 8 input parameters, corresponding to the XGBoost hyperparameters. Table 4 shows the hyperparameters optimised in the three Profet benchmark problems (Klein et al., 2019), their search spaces, and whether or not they were log scaled. Like the other optimisation runs performed in this work, the inputs are rescaled to reside in $[0, 1]$. Figure 5 shows the average rank score plots for the three functions.

Table 4: Parameters tuned in the Profet benchmark.

Benchmark	Parameter Name	Range	Log scaled
SVM	C	$[e^{-10}, e^{10}]$	Yes
	γ	$[e^{-10}, e^{10}]$	Yes
FC-NET	Learning rate	$[10^{-6}, 10^{-1}]$	Yes
	Batch size	$[2^3, 2^7]$	Yes
	Layer 1: Units	$[2^4, 2^9]$	Yes
	Layer 2: Units	$[2^4, 2^9]$	Yes
	Layer 1: dropout rate	$[0, 0.99]$	-
	Layer 2: dropout rate	$[0, 0.99]$	-
XGBoost	Learning rate	$[10^{-6}, 10^{-1}]$	Yes
	γ	$[0, 2]$	-
	L1 regularisation	$[10^{-5}, 10^3]$	Yes
	L2 regularisation	$[10^{-5}, 10^3]$	Yes
	Number of estimators	$[10, 500]$	-
	Subsampling	$[0.1, 1]$	-
	Maximum depth	$[1, 15]$	-
	Minimum child weight	$[0, 20]$	-

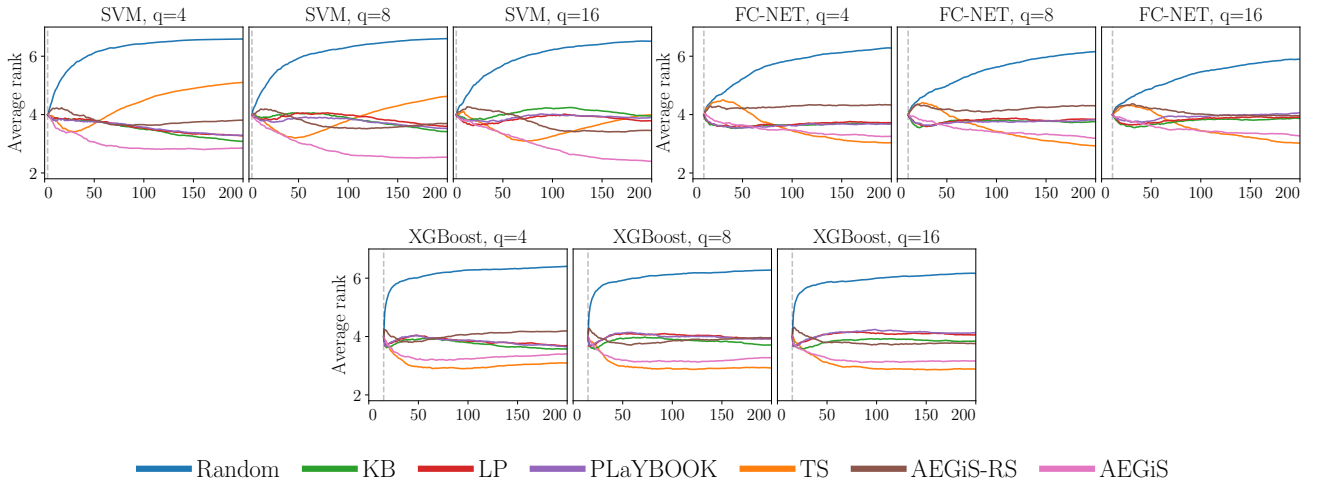


Figure 5: Average rank scores for the SVM, FC-NET and XGBoost hyperparameter optimisation problems.

3.2 Robot Pushing Problems

Here, we optimised the control parameters for two active learning robot pushing problems. In the first problem (push4), a robot hand is given the task of pushing an object towards an unknown target location. Once the robot has finished pushing the object, it receives feedback in the form of the object-target distance. The adjustable parameters in this problem are the robot’s starting coordinates on the $2d$ plain, the orientation of its hand and how long it pushes for. Therefore, this problem can be cast as a minimisation in which we optimise the four parameters in order to minimise the object-target distance. The object’s initial location in push4 is always the centre of the domain, and for each problem instance the target location is randomly generated. Note that these instances are shared between methods.

The second problem (push8) is similar to the first except there are two robots moving in the same arena, both having to push their own objects to their respective targets. The final object-target distance from both robots are summed to give an objective function to minimise, resulting in an 8-dimensional problem. Problem instances for push8 were generated such that the minimum distance between the targets was sufficient that each of the objects could be placed on the targets without overlapping. However, this does not mean that each problem instance can be successfully optimised because the targets may be positioned such that the robots block each others path *en route* to the target location.

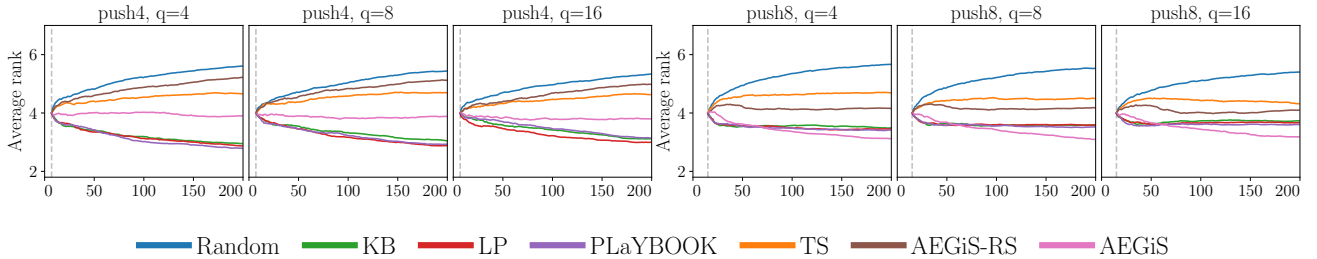


Figure 6: Average rank scores for the push4 and push8 problems.

4 Ablation Study

In this section we show all convergence plots and results tables for the ablation study on AEGiS using the synthetic functions. Figure 7 shows the convergence plots for each of the six methods on the fifteen benchmark problems for $q \in \{4, 8, 16\}$. Each plot shows the median log simple regret, with shading representing the interquartile range over 51 runs. Tables 5, 6 and 7 show the median log simple regret as well as the median absolute deviation from the median (MAD), a robust measure of dispersion. The method with the best (lowest) median regret is shown in dark grey, and those that are statistically equivalent to the best method according to a one-sided, paired Wilcoxon signed-rank test with Holm-Bonferroni correction (Holm, 1979) ($p \geq 0.05$) are shown in light grey.

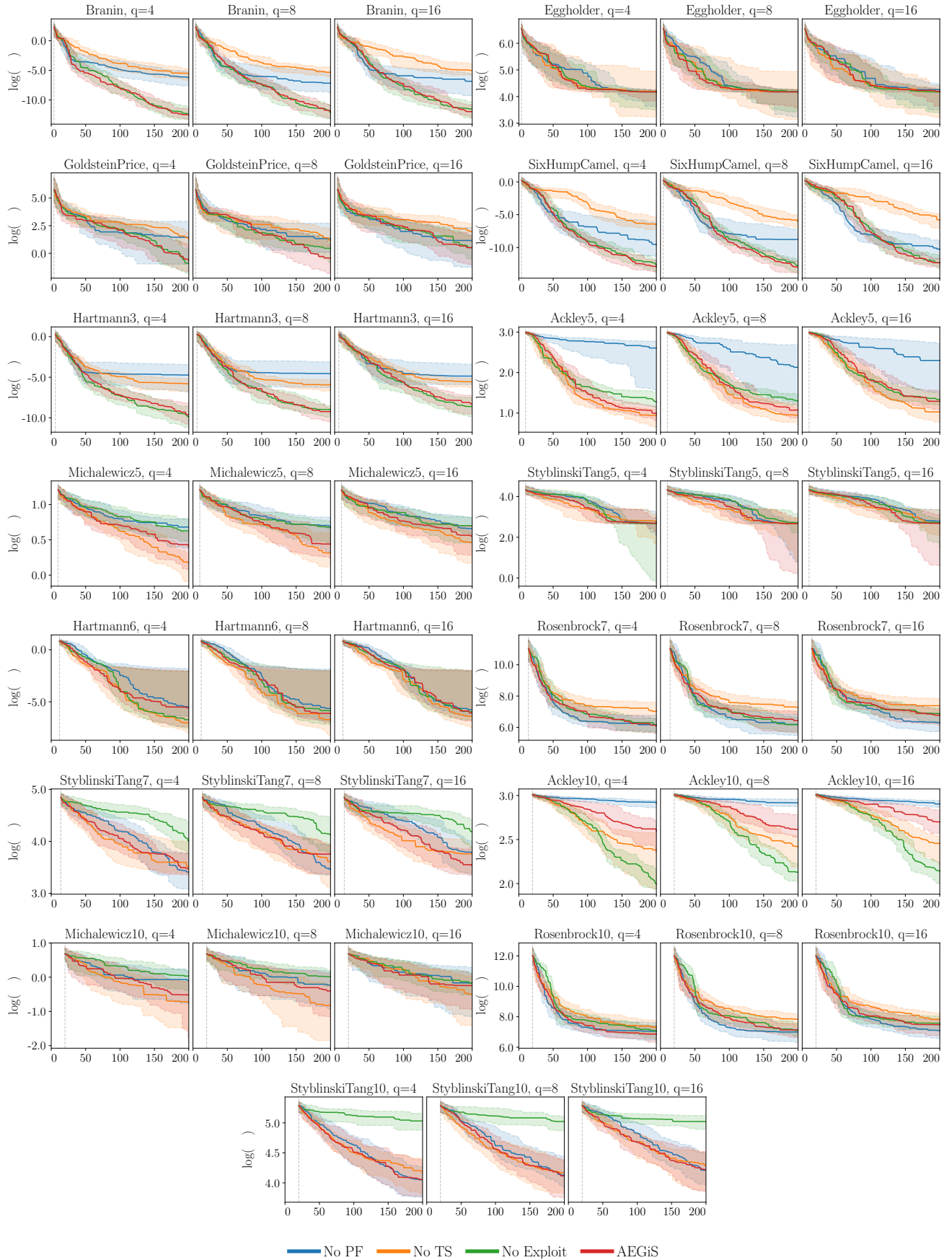


Figure 7: Convergence results for the ablation study.

Table 5: Tabulated results for $q = 4$ asynchronous workers, showing the median log simple regret (*left*) and median absolute deviation from the median (MAD, *right*) after 200 function evaluations across the 51 runs. The method with the lowest median performance is shown in dark grey, with those with statistically equivalent performance are shown in light grey.

Method	Branin (2)		Eggholder (2)		GoldsteinPrice (2)		SixHumpCamel (2)		Hartmann3 (3)	
	Median	MAD	Median	MAD	Median	MAD	Median	MAD	Median	MAD
No PF	1.87×10^{-3}	2.58×10^{-3}	6.51×10^1	1.80×10^1	4.24	6.26	7.00×10^{-5}	1.03×10^{-4}	8.84×10^{-3}	1.22×10^{-2}
No TS	3.78×10^{-3}	4.51×10^{-3}	6.63×10^1	8.79×10^1	3.64	3.73	1.50×10^{-3}	1.77×10^{-3}	2.97×10^{-3}	2.78×10^{-3}
No Exploit	4.20×10^{-6}	4.73×10^{-6}	6.51×10^1	1.74×10^1	4.08×10^{-1}	5.43×10^{-1}	3.22×10^{-6}	4.12×10^{-6}	5.30×10^{-5}	6.79×10^{-5}
AEGiS	3.82×10^{-6}	4.67×10^{-6}	6.51×10^1	8.35	5.09×10^{-1}	6.15×10^{-1}	2.53×10^{-6}	2.82×10^{-6}	6.73×10^{-5}	8.80×10^{-5}
Method	Ackley5 (5)		Michalewicz5 (5)		StyblinskiTang5 (5)		Hartmann6 (6)		Rosenbrock7 (7)	
	Median	MAD	Median	MAD	Median	MAD	Median	MAD	Median	MAD
No PF	1.36×10^1	4.78	1.98	4.16×10^{-1}	1.47×10^1	1.47×10^1	4.20×10^{-3}	5.19×10^{-3}	4.76×10^2	3.30×10^2
No TS	2.56	7.91×10^{-1}	1.19	3.18×10^{-1}	1.63×10^1	1.13×10^1	8.95×10^{-4}	1.13×10^{-3}	1.12×10^3	7.51×10^2
No Exploit	3.61	9.86×10^{-1}	1.87	4.42×10^{-1}	1.45×10^1	1.73×10^1	1.21×10^{-3}	1.50×10^{-3}	4.50×10^2	2.59×10^2
AEGiS	2.70	6.70×10^{-1}	1.48	5.05×10^{-1}	1.47×10^1	6.34	3.76×10^{-3}	5.26×10^{-3}	4.47×10^2	3.45×10^2
Method	StyblinskiTang7 (7)		Ackley10 (10)		Michalewicz10 (10)		Rosenbrock10 (10)		StyblinskiTang10 (10)	
	Median	MAD	Median	MAD	Median	MAD	Median	MAD	Median	MAD
No PF	3.02×10^1	1.95×10^1	1.85×10^1	1.09	9.14×10^{-1}	5.40×10^{-1}	1.15×10^3	9.62×10^2	5.74×10^1	2.10×10^1
No TS	3.36×10^1	2.25×10^1	1.08×10^1	3.93	4.66×10^{-1}	5.42×10^{-1}	1.53×10^3	8.32×10^2	6.39×10^1	2.64×10^1
No Exploit	5.46×10^1	2.71×10^1	7.38	1.39	1.03	4.58×10^{-1}	1.18×10^3	7.14×10^2	1.53×10^2	3.35×10^1
AEGiS	3.21×10^1	1.61×10^1	1.34×10^1	2.80	5.87×10^{-1}	5.78×10^{-1}	9.45×10^2	7.03×10^2	5.78×10^1	3.10×10^1

Table 6: Tabulated results for $q = 8$ asynchronous workers, showing the median log simple regret (*left*) and median absolute deviation from the median (MAD, *right*) after 200 function evaluations across the 51 runs. The method with the lowest median performance is shown in dark grey, with those with statistically equivalent performance are shown in light grey.

Method	Branin (2)		Eggholder (2)		GoldsteinPrice (2)		SixHumpCamel (2)		Hartmann3 (3)	
	Median	MAD	Median	MAD	Median	MAD	Median	MAD	Median	MAD
No PF	7.73×10^{-4}	1.14×10^{-3}	6.51×10^1	3.39×10^1	3.78	5.46	1.55×10^{-4}	2.26×10^{-4}	1.05×10^{-2}	1.44×10^{-2}
No TS	4.90×10^{-3}	5.69×10^{-3}	6.54×10^1	7.27×10^1	3.26	3.61	2.44×10^{-3}	2.86×10^{-3}	2.60×10^{-3}	2.39×10^{-3}
No Exploit	5.28×10^{-6}	6.77×10^{-6}	6.60×10^1	2.61×10^1	1.56	1.95	2.94×10^{-6}	3.49×10^{-6}	1.26×10^{-4}	1.13×10^{-4}
AEGiS	7.10×10^{-6}	8.66×10^{-6}	6.51×10^1	2.76×10^1	6.48×10^{-1}	8.22×10^{-1}	2.35×10^{-6}	2.83×10^{-6}	9.71×10^{-5}	9.88×10^{-5}
Method	Ackley5 (5)		Michalewicz5 (5)		StyblinskiTang5 (5)		Hartmann6 (6)		Rosenbrock7 (7)	
	Median	MAD	Median	MAD	Median	MAD	Median	MAD	Median	MAD
No PF	8.41	8.03	2.00	4.95×10^{-1}	1.44×10^1	3.17	3.54×10^{-3}	4.78×10^{-3}	4.85×10^2	4.39×10^2
No TS	2.58	7.86×10^{-1}	1.37	4.58×10^{-1}	1.44×10^1	1.23×10^1	1.22×10^{-3}	1.60×10^{-3}	1.46×10^3	9.07×10^2
No Exploit	3.68	7.93×10^{-1}	1.96	3.87×10^{-1}	1.51×10^1	1.31×10^1	2.83×10^{-3}	3.96×10^{-3}	4.79×10^2	3.09×10^2
AEGiS	2.92	7.50×10^{-1}	1.55	5.89×10^{-1}	1.44×10^1	1.79×10^1	2.23×10^{-3}	2.71×10^{-3}	6.19×10^2	5.82×10^2
Method	StyblinskiTang7 (7)		Ackley10 (10)		Michalewicz10 (10)		Rosenbrock10 (10)		StyblinskiTang10 (10)	
	Median	MAD	Median	MAD	Median	MAD	Median	MAD	Median	MAD
No PF	3.20×10^1	1.80×10^1	1.85×10^1	1.09	7.95×10^{-1}	5.89×10^{-1}	1.09×10^3	7.33×10^2	6.22×10^1	2.28×10^1
No TS	3.70×10^1	2.21×10^1	1.12×10^1	2.31	4.40×10^{-1}	4.86×10^{-1}	2.55×10^3	1.58×10^3	6.46×10^1	2.72×10^1
No Exploit	6.21×10^1	3.51×10^1	8.39	1.34	1.02	3.30×10^{-1}	1.22×10^3	6.31×10^2	1.52×10^2	2.54×10^1
AEGiS	4.27×10^1	1.98×10^1	1.37×10^1	2.93	6.68×10^{-1}	6.68×10^{-1}	1.26×10^3	7.68×10^2	6.14×10^1	2.79×10^1

Table 7: Tabulated results for $q = 16$ asynchronous workers, showing the median log simple regret (*left*) and median absolute deviation from the median (MAD, *right*) after 200 function evaluations across the 51 runs. The method with the lowest median performance is shown in dark grey, with those with statistically equivalent performance are shown in light grey.

Method	Branin (2)		Eggholder (2)		GoldsteinPrice (2)		SixHumpCamel (2)		Hartmann3 (3)	
	Median	MAD	Median	MAD	Median	MAD	Median	MAD	Median	MAD
No PF	1.06×10^{-3}	1.55×10^{-3}	7.07×10^1	4.58×10^1	3.19	4.63	3.56×10^{-5}	4.69×10^{-5}	7.75×10^{-3}	1.13×10^{-2}
No TS	6.67×10^{-3}	7.63×10^{-3}	6.51×10^1	5.92×10^1	7.21	8.09	3.09×10^{-3}	4.11×10^{-3}	3.86×10^{-3}	2.95×10^{-3}
No Exploit	1.01×10^{-5}	1.36×10^{-5}	6.51×10^1	3.15×10^1	1.65	2.05	4.54×10^{-6}	5.45×10^{-6}	1.83×10^{-4}	2.41×10^{-4}
AEGiS	5.88×10^{-6}	8.01×10^{-6}	6.54×10^1	1.49×10^1	1.67	2.27	4.40×10^{-6}	4.38×10^{-6}	2.53×10^{-4}	3.04×10^{-4}

Method	Ackley5 (5)		Michalewicz5 (5)		StyblinskiTang5 (5)		Hartmann6 (6)		Rosenbrock7 (7)	
	Median	MAD	Median	MAD	Median	MAD	Median	MAD	Median	MAD
No PF	9.98	8.05	1.93	2.98×10^{-1}	1.63×10^1	1.82×10^1	3.16×10^{-3}	3.50×10^{-3}	5.44×10^2	4.00×10^2
No TS	2.80	9.83×10^{-1}	1.59	4.78×10^{-1}	1.47×10^1	1.23×10^1	1.66×10^{-3}	1.90×10^{-3}	1.61×10^3	1.13×10^3
No Exploit	3.80	7.76×10^{-1}	1.99	4.63×10^{-1}	1.51×10^1	6.02	2.62×10^{-3}	3.46×10^{-3}	9.71×10^2	6.76×10^2
AEGiS	3.64	1.30	1.73	4.50×10^{-1}	1.47×10^1	1.86×10^1	2.25×10^{-3}	2.70×10^{-3}	8.72×10^2	6.23×10^2

Method	StyblinskiTang7 (7)		Ackley10 (10)		Michalewicz10 (10)		Rosenbrock10 (10)		StyblinskiTang10 (10)	
	Median	MAD	Median	MAD	Median	MAD	Median	MAD	Median	MAD
No PF	4.35×10^1	2.08×10^1	1.83×10^1	9.93×10^{-1}	8.46×10^{-1}	7.68×10^{-1}	1.20×10^3	8.13×10^2	6.75×10^1	2.87×10^1
No TS	4.29×10^1	1.89×10^1	1.17×10^1	2.85	6.04×10^{-1}	5.47×10^{-1}	2.53×10^3	1.45×10^3	7.29×10^1	3.20×10^1
No Exploit	6.58×10^1	2.60×10^1	8.50	1.54	8.40×10^{-1}	4.16×10^{-1}	1.95×10^3	1.27×10^3	1.52×10^2	2.42×10^1
AEGiS	3.37×10^1	1.93×10^1	1.49×10^1	2.99	7.84×10^{-1}	5.67×10^{-1}	1.77×10^3	1.13×10^3	6.81×10^1	3.26×10^1

5 Selecting ϵ

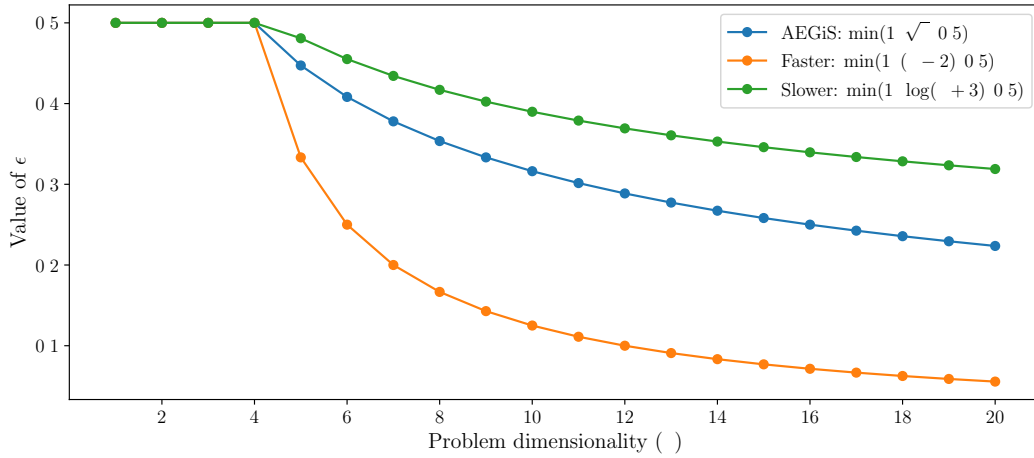


Figure 8: Epsilon decay rate for the three evaluated heuristics. Here, *faster* refers to a higher rate of decay and thus more exploitation, whereas *slower* refers to a lower rate of decay and therefore more exploration.

In this section we show all convergence plots and results table for choosing a suitable value of ϵ . Here, AEGiS corresponds to the value used throughout the rest of the paper, $\epsilon = \min(1/\sqrt{d}, 1/2)$. The labels *faster* and *slower* correspond to using values of $\epsilon = \min(1/(d-2), 1/2)$ and $\epsilon = \min(1/\log(d+3), 1/2)$ respectively, where *faster* and *slower* refer to the increased and decrease rate of decay of ϵ with respect to the problem dimensionality d . Therefore, *faster* exploits more than AEGiS, and *slower* explores more than AEGiS for a given problem dimensionality. Figure 8 shows the three ϵ decay curves. Figure 9 shows the convergence plots for AEGiS with the three ϵ decay rates evaluated on the 15 synthetic test functions for $q \in \{4, 8, 16\}$. Tables 8, 9, and 10 show the median log simple regret as well as the median absolute deviation from the median (MAD), a robust measure of dispersion. The method with the best (lowest) median regret is shown in dark grey, and those that are statistically equivalent to the best method according to a one-sided, paired Wilcoxon signed-rank test with Holm-Bonferroni correction (Holm, 1979) ($p \geq 0.05$) are shown in light grey.

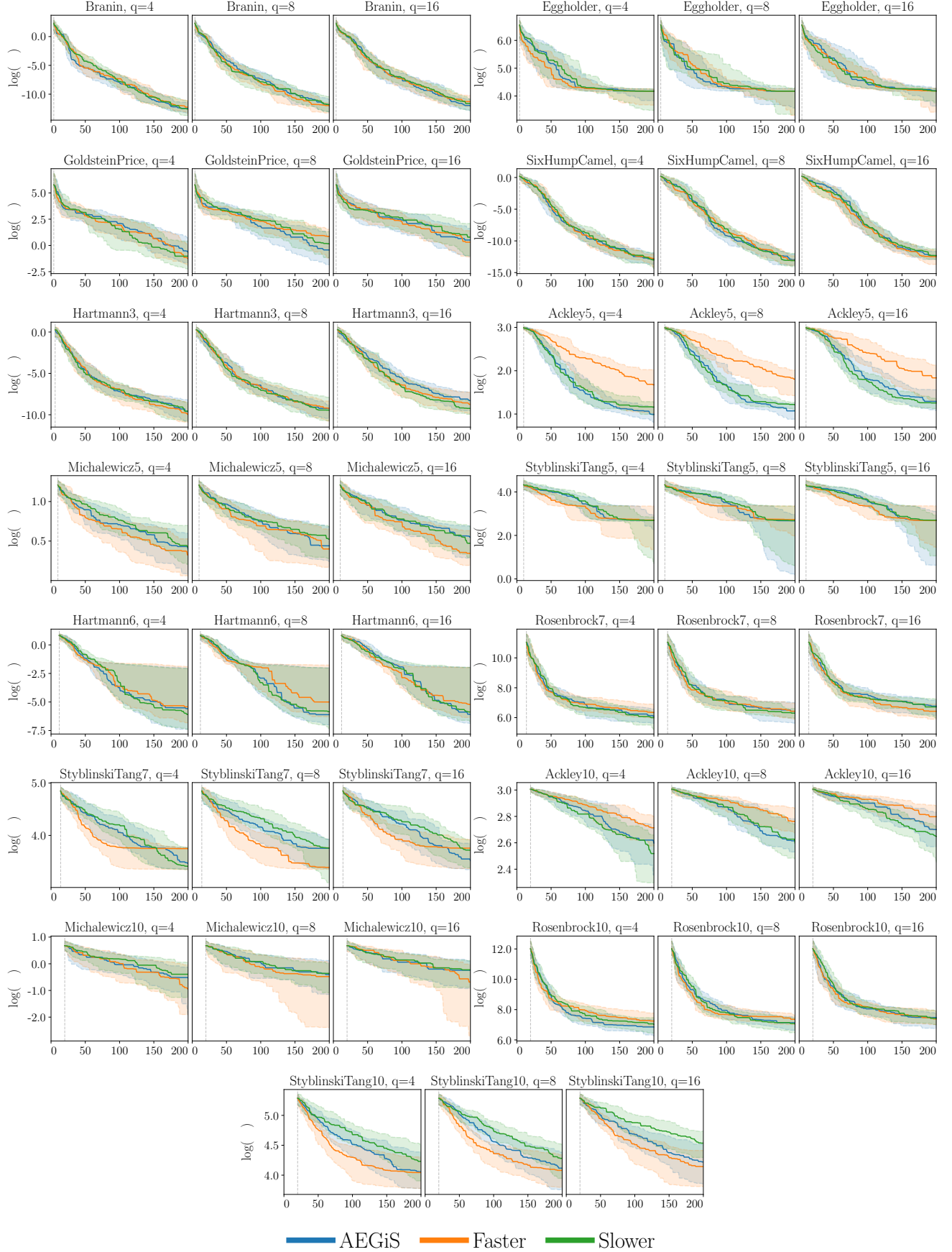


Figure 9: Convergence results for the ϵ value experiments.

Table 8: Tabulated results for $q = 4$ asynchronous workers, showing the median log simple regret (*left*) and median absolute deviation from the median (MAD, *right*) after 200 function evaluations across the 51 runs. The method with the lowest median performance is shown in dark grey, with those with statistically equivalent performance are shown in light grey.

Method	Branin (2)		Eggholder (2)		GoldsteinPrice (2)		SixHumpCamel (2)		Hartmann3 (3)	
	Median	MAD	Median	MAD	Median	MAD	Median	MAD	Median	MAD
AEGiS	3.82×10^{-6}	4.67×10^{-6}	6.51×10^1	8.35	5.09×10^{-1}	6.15×10^{-1}	2.53×10^{-6}	2.82×10^{-6}	6.73×10^{-5}	8.80×10^{-5}
Faster	4.81×10^{-6}	5.56×10^{-6}	6.51×10^1	1.10×10^1	2.84×10^{-1}	3.57×10^{-1}	2.83×10^{-6}	3.17×10^{-6}	4.76×10^{-5}	5.89×10^{-5}
Slower	3.47×10^{-6}	4.18×10^{-6}	6.51×10^1	1.61×10^1	3.60×10^{-1}	4.71×10^{-1}	2.25×10^{-6}	2.87×10^{-6}	7.01×10^{-5}	8.80×10^{-5}
Method	Ackley5 (5)		Michalewicz5 (5)		StyblinskiTang5 (5)		Hartmann6 (6)		Rosenbrock7 (7)	
	Median	MAD	Median	MAD	Median	MAD	Median	MAD	Median	MAD
AEGiS	2.70	6.70×10^{-1}	1.48	5.05×10^{-1}	1.47×10^1	6.34	3.76×10^{-3}	5.26×10^{-3}	4.47×10^2	3.45×10^2
Faster	5.34	3.53	1.38	4.77×10^{-1}	1.50×10^1	1.99×10^1	4.41×10^{-3}	6.05×10^{-3}	5.72×10^2	3.43×10^2
Slower	3.20	6.71×10^{-1}	1.53	6.13×10^{-1}	1.47×10^1	1.32×10^1	2.28×10^{-3}	3.07×10^{-3}	4.04×10^2	3.08×10^2
Method	StyblinskiTang7 (7)		Ackley10 (10)		Michalewicz10 (10)		Rosenbrock10 (10)		StyblinskiTang10 (10)	
	Median	MAD	Median	MAD	Median	MAD	Median	MAD	Median	MAD
AEGiS	3.21×10^1	1.61×10^1	1.34×10^1	2.80	5.87×10^{-1}	5.78×10^{-1}	9.45×10^2	7.03×10^2	5.78×10^1	3.10×10^1
Faster	4.25×10^1	2.04×10^1	1.51×10^1	2.52	3.91×10^{-1}	5.00×10^{-1}	1.40×10^3	9.75×10^2	5.70×10^1	2.25×10^1
Slower	3.03×10^1	1.93×10^1	1.24×10^1	3.37	6.75×10^{-1}	5.70×10^{-1}	1.13×10^3	8.73×10^2	6.87×10^1	3.00×10^1

Table 9: Tabulated results for $q = 8$ asynchronous workers, showing the median log simple regret (*left*) and median absolute deviation from the median (MAD, *right*) after 200 function evaluations across the 51 runs. The method with the lowest median performance is shown in dark grey, with those with statistically equivalent performance are shown in light grey.

Method	Branin (2)		Eggholder (2)		GoldsteinPrice (2)		SixHumpCamel (2)		Hartmann3 (3)	
	Median	MAD	Median	MAD	Median	MAD	Median	MAD	Median	MAD
AEGiS	7.10×10^{-6}	8.66×10^{-6}	6.51×10^1	2.76×10^1	6.48×10^{-1}	8.22×10^{-1}	2.35×10^{-6}	2.83×10^{-6}	9.71×10^{-5}	9.88×10^{-5}
Faster	5.96×10^{-6}	6.64×10^{-6}	6.51×10^1	1.42×10^1	2.36	3.10	2.09×10^{-6}	2.07×10^{-6}	9.89×10^{-5}	1.16×10^{-4}
Slower	7.57×10^{-6}	1.02×10^{-5}	6.51×10^1	2.30×10^1	1.16	1.62	2.02×10^{-6}	2.63×10^{-6}	7.94×10^{-5}	9.45×10^{-5}
Method	Ackley5 (5)		Michalewicz5 (5)		StyblinskiTang5 (5)		Hartmann6 (6)		Rosenbrock7 (7)	
	Median	MAD	Median	MAD	Median	MAD	Median	MAD	Median	MAD
AEGiS	2.92	7.50×10^{-1}	1.55	5.89×10^{-1}	1.44×10^1	1.79×10^1	2.23×10^{-3}	2.71×10^{-3}	6.19×10^2	5.82×10^2
Faster	6.09	2.54	1.49	5.13×10^{-1}	1.53×10^1	1.94×10^1	6.73×10^{-3}	9.57×10^{-3}	6.20×10^2	4.57×10^2
Slower	3.37	6.10×10^{-1}	1.69	5.22×10^{-1}	1.47×10^1	2.03×10^1	2.91×10^{-3}	4.06×10^{-3}	5.45×10^2	2.68×10^2
Method	StyblinskiTang7 (7)		Ackley10 (10)		Michalewicz10 (10)		Rosenbrock10 (10)		StyblinskiTang10 (10)	
	Median	MAD	Median	MAD	Median	MAD	Median	MAD	Median	MAD
AEGiS	4.27×10^1	1.98×10^1	1.37×10^1	2.93	6.68×10^{-1}	6.68×10^{-1}	1.26×10^3	7.68×10^2	6.14×10^1	2.79×10^1
Faster	2.96×10^1	1.94×10^1	1.58×10^1	2.13	6.19×10^{-1}	7.61×10^{-1}	1.57×10^3	6.94×10^2	5.92×10^1	2.36×10^1
Slower	4.29×10^1	1.85×10^1	1.34×10^1	2.84	6.98×10^{-1}	4.79×10^{-1}	1.14×10^3	8.00×10^2	7.23×10^1	2.85×10^1

Table 10: Tabulated results for $q = 16$ asynchronous workers, showing the median log simple regret (*left*) and median absolute deviation from the median (MAD, *right*) after 200 function evaluations across the 51 runs. The method with the lowest median performance is shown in dark grey, with those with statistically equivalent performance are shown in light grey.

Method	Branin (2)		Eggholder (2)		GoldsteinPrice (2)		SixHumpCamel (2)		Hartmann3 (3)	
	Median	MAD	Median	MAD	Median	MAD	Median	MAD	Median	MAD
AEGiS	5.88×10^{-6}	8.01×10^{-6}	6.54×10^1	1.49×10^1	1.67	2.27	4.40×10^{-6}	4.38×10^{-6}	2.53×10^{-4}	3.04×10^{-4}
Faster	1.26×10^{-5}	1.55×10^{-5}	6.54×10^1	1.32×10^1	1.36	1.92	3.71×10^{-6}	4.40×10^{-6}	1.61×10^{-4}	1.92×10^{-4}
Slower	9.08×10^{-6}	9.72×10^{-6}	6.54×10^1	1.73×10^1	2.20	3.04	4.51×10^{-6}	5.24×10^{-6}	9.79×10^{-5}	1.17×10^{-4}

Method	Ackley5 (5)		Michalewicz5 (5)		StyblinskiTang5 (5)		Hartmann6 (6)		Rosenbrock7 (7)	
	Median	MAD	Median	MAD	Median	MAD	Median	MAD	Median	MAD
AEGiS	3.64	1.30	1.73	4.50×10^{-1}	1.47×10^1	1.86×10^1	2.25×10^{-3}	2.70×10^{-3}	8.72×10^2	6.23×10^2
Faster	6.26	3.70	1.41	5.64×10^{-1}	1.46×10^1	2.03×10^1	5.44×10^{-3}	7.27×10^{-3}	6.18×10^2	5.03×10^2
Slower	3.51	6.31×10^{-1}	1.60	4.95×10^{-1}	1.49×10^1	1.74×10^1	2.82×10^{-3}	3.14×10^{-3}	8.27×10^2	7.18×10^2

Method	StyblinskiTang7 (7)		Ackley10 (10)		Michalewicz10 (10)		Rosenbrock10 (10)		StyblinskiTang10 (10)	
	Median	MAD	Median	MAD	Median	MAD	Median	MAD	Median	MAD
AEGiS	3.37×10^1	1.93×10^1	1.49×10^1	2.99	7.84×10^{-1}	5.67×10^{-1}	1.77×10^3	1.13×10^3	6.81×10^1	3.26×10^1
Faster	4.28×10^1	2.04×10^1	1.64×10^1	2.21	5.04×10^{-1}	6.68×10^{-1}	1.61×10^3	1.12×10^3	6.30×10^1	2.76×10^1
Slower	4.12×10^1	1.62×10^1	1.41×10^1	2.44	7.98×10^{-1}	5.26×10^{-1}	1.67×10^3	1.11×10^3	9.33×10^1	2.98×10^1

6 Sequential Bayesian Optimisation ($q = 1$)

In this section we evaluate AEGiS in the sequential BO setting, i.e. with $q = 1$ workers and compare it to the other asynchronous methods in Section 6.1, carry out an ablation study in Section 6.2 and investigate faster and slower ϵ decay rates in Section 6.3.

6.1 Evaluation

We first compare AEGiS to the other asynchronous methods in the sequential setting. Note that KB, LP and PLAYBOOK are equivalent because each select the first location to be evaluated using EI. Therefore, we compare AEGiS and AEGiS-RS to EI, TS and Latin hypercube sampling (i.e. Random) on the 15 synthetic benchmark functions. Figure 10 shows the convergence plots for the benchmark functions, with solid lines showing the median log simple regret and shading showing the interquartile range. Table 11, show the median log simple regret as well as the median absolute deviation from the median (MAD), a robust measure of dispersion. The method with the best (lowest) median regret is shown in dark grey, and those that are statistically equivalent to the best method according to a one-sided, paired Wilcoxon signed-rank test with Holm-Bonferroni correction (Holm, 1979) ($p \geq 0.05$) are shown in light grey. Figure 11 summarises the tabulated results and shows the number of times each method is best or statistically equal to the best performing method.

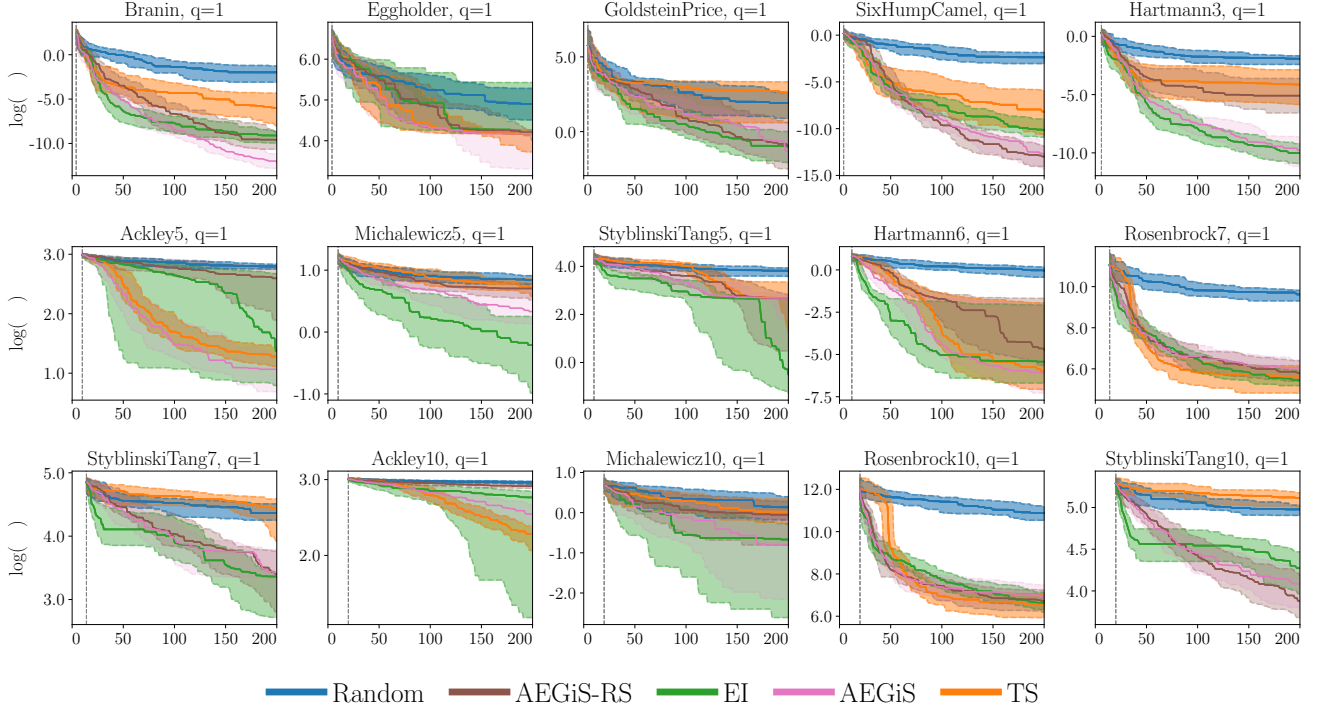


Figure 10: Convergence results for the sequential BO experiments.

Table 11: Tabulated results for the sequential ($q = 1$) BO optimisation runs, showing the median log simple regret (*left*) and median absolute deviation from the median (MAD, *right*) after 200 function evaluations across the 51 runs. The method with the lowest median performance is shown in dark grey, with those with statistically equivalent performance are shown in light grey.

Method	Branin (2)		Eggholder (2)		GoldsteinPrice (2)		SixHumpCamel (2)		Hartmann3 (3)	
	Median	MAD	Median	MAD	Median	MAD	Median	MAD	Median	MAD
Random	1.37×10^{-1}	1.41×10^{-1}	1.35×10^2	7.08×10^1	6.75	7.57	9.30×10^{-2}	7.41×10^{-2}	1.46×10^{-1}	7.08×10^{-2}
TS	2.51×10^{-3}	3.58×10^{-3}	6.51×10^1	1.13×10^1	1.32×10^1	1.91×10^1	2.81×10^{-4}	4.14×10^{-4}	1.59×10^{-2}	2.15×10^{-2}
EI	1.11×10^{-4}	9.39×10^{-5}	6.71×10^1	9.25	3.46×10^{-1}	4.25×10^{-1}	3.87×10^{-5}	4.74×10^{-5}	4.42×10^{-5}	4.74×10^{-5}
AEGiS-RS	6.76×10^{-5}	9.41×10^{-5}	6.58×10^1	7.47	3.96×10^{-1}	5.23×10^{-1}	2.30×10^{-6}	2.64×10^{-6}	6.16×10^{-3}	8.59×10^{-3}
AEGiS	5.69×10^{-6}	4.87×10^{-6}	6.51×10^1	2.09×10^1	2.71×10^{-1}	3.67×10^{-1}	3.08×10^{-6}	3.94×10^{-6}	5.62×10^{-5}	6.94×10^{-5}
Method	Ackley5 (5)		Michalewicz5 (5)		StyblinskiTang5 (5)		Hartmann6 (6)		Rosenbrock7 (7)	
	Median	MAD	Median	MAD	Median	MAD	Median	MAD	Median	MAD
Random	1.64×10^1	1.01	2.32	2.49×10^{-1}	4.56×10^1	1.32×10^1	9.51×10^{-1}	4.03×10^{-1}	1.51×10^4	4.90×10^3
TS	3.59	8.21×10^{-1}	2.07	4.32×10^{-1}	1.45×10^1	1.94×10^1	2.44×10^{-3}	2.89×10^{-3}	2.68×10^2	2.35×10^2
EI	3.94	4.60	8.09×10^{-1}	6.85×10^{-1}	6.13×10^{-1}	7.75×10^{-1}	4.40×10^{-3}	5.64×10^{-3}	2.33×10^2	1.19×10^2
AEGiS-RS	1.34×10^1	6.18	2.02	3.77×10^{-1}	1.46×10^1	1.09×10^1	8.86×10^{-3}	1.16×10^{-2}	3.24×10^2	2.10×10^2
AEGiS	2.90	1.44	1.39	5.38×10^{-1}	1.46×10^1	2.95	2.21×10^{-3}	2.77×10^{-3}	4.20×10^2	2.33×10^2
Method	StyblinskiTang7 (7)		Ackley10 (10)		Michalewicz10 (10)		Rosenbrock10 (10)		StyblinskiTang10 (10)	
	Median	MAD	Median	MAD	Median	MAD	Median	MAD	Median	MAD
Random	7.85×10^1	1.81×10^1	1.93×10^1	4.99×10^{-1}	1.14	4.75×10^{-1}	5.32×10^4	2.30×10^4	1.45×10^2	1.46×10^1
TS	8.48×10^1	2.92×10^1	9.82	2.18	1.02	5.10×10^{-1}	6.98×10^2	5.45×10^2	1.66×10^2	2.04×10^1
EI	2.89×10^1	1.74×10^1	1.59×10^1	4.32	5.12×10^{-1}	5.58×10^{-1}	7.59×10^2	3.91×10^2	7.18×10^1	2.66×10^1
AEGiS-RS	3.00×10^1	1.93×10^1	1.84×10^1	6.36×10^{-1}	9.48×10^{-1}	6.22×10^{-1}	8.23×10^2	5.14×10^2	4.85×10^1	1.96×10^1
AEGiS	3.07×10^1	1.89×10^1	1.27×10^1	2.38	4.46×10^{-1}	5.98×10^{-1}	1.03×10^3	7.26×10^2	5.95×10^1	2.10×10^1

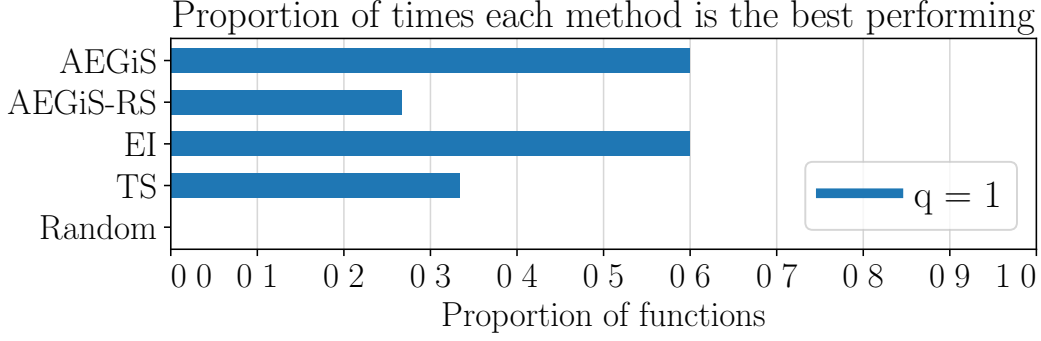


Figure 11: Synthetic function optimisation summary. Bar lengths correspond to the proportion of times that a method is best or statistically equivalent to the best method across the 15 synthetic functions.

6.2 Ablation Study

Next, we perform an ablation study as before in the main paper. Figure 12 shows the convergence plots for the benchmark functions, with solid lines showing the median log simple regret and shading showing the interquartile range. Table 12, show the median log simple regret as well as the median absolute deviation from the median (MAD), a robust measure of dispersion. The method with the best (lowest) median regret is shown in dark grey, and those that are statistically equivalent to the best method according to a one-sided, paired Wilcoxon signed-rank test with Holm-Bonferroni correction (Holm, 1979) ($p \geq 0.05$) are shown in light grey. Figure 13 summarises the tabulated results and shows the number of times each method is best or statistically equal to the best performing method.

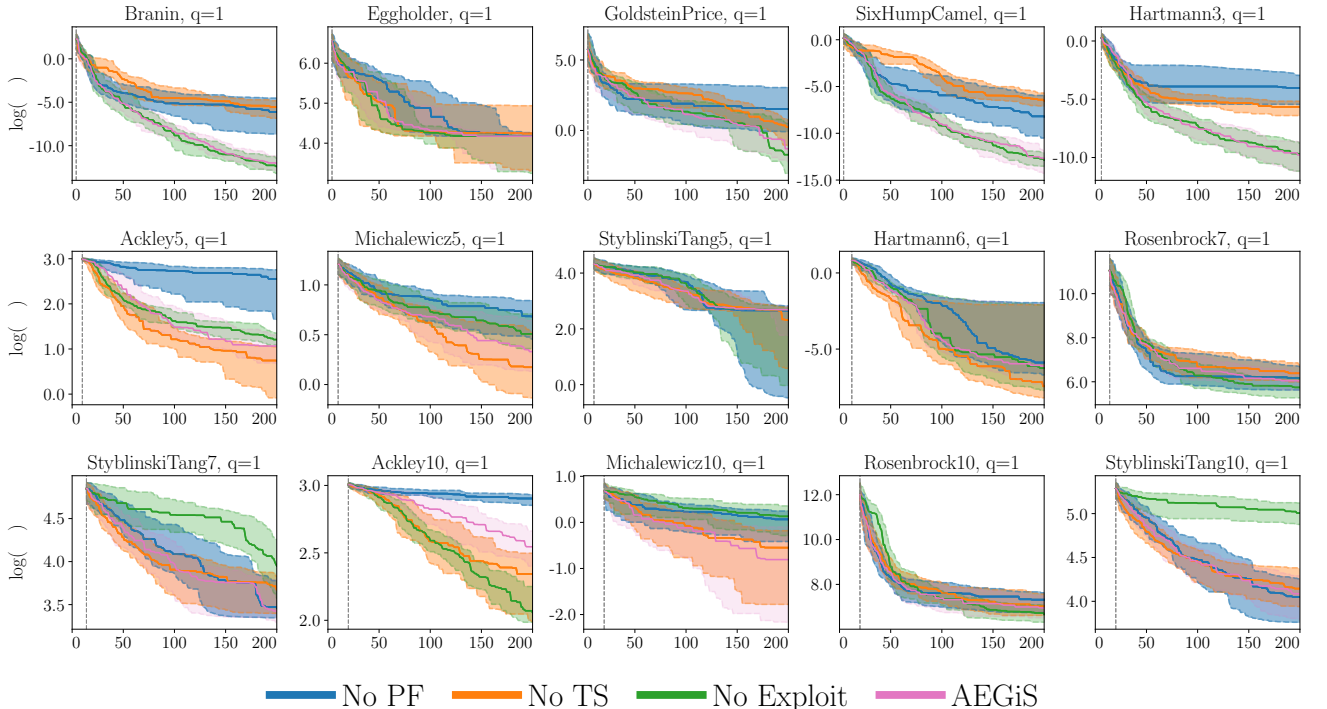


Figure 12: Convergence results for the ablation study experiments.

Table 12: Tabulated results for the ablation study of the sequential ($q = 1$) BO optimisation runs, showing the median log simple regret (*left*) and median absolute deviation from the median (MAD, *right*) after 200 function evaluations across the 51 runs. The method with the lowest median performance is shown in dark grey, with those with statistically equivalent performance are shown in light grey.

Method	Branin (2)		Eggholder (2)		GoldsteinPrice (2)		SixHumpCamel (2)		Hartmann3 (3)	
	Median	MAD	Median	MAD	Median	MAD	Median	MAD	Median	MAD
No PF	2.24×10^{-3}	3.28×10^{-3}	6.51×10^1	8.41	4.54	6.51	2.73×10^{-4}	4.01×10^{-4}	1.75×10^{-2}	2.20×10^{-2}
No TS	3.85×10^{-3}	4.64×10^{-3}	6.96×10^1	8.70×10^1	1.28	1.36	1.47×10^{-3}	1.41×10^{-3}	3.43×10^{-3}	2.87×10^{-3}
No Exploit	4.20×10^{-6}	4.25×10^{-6}	6.51×10^1	1.32×10^1	1.79×10^{-1}	2.50×10^{-1}	2.59×10^{-6}	2.57×10^{-6}	6.05×10^{-5}	7.30×10^{-5}
AEGiS	5.69×10^{-6}	4.87×10^{-6}	6.51×10^1	2.09×10^1	2.71×10^{-1}	3.67×10^{-1}	3.08×10^{-6}	3.94×10^{-6}	5.62×10^{-5}	6.94×10^{-5}

Method	Ackley5 (5)		Michalewicz5 (5)		StyblinskiTang5 (5)		Hartmann6 (6)		Rosenbrock7 (7)	
	Median	MAD	Median	MAD	Median	MAD	Median	MAD	Median	MAD
No PF	1.29×10^1	5.68	1.98	5.14×10^{-1}	1.43×10^1	2.00×10^1	2.78×10^{-3}	3.38×10^{-3}	4.73×10^2	3.39×10^2
No TS	2.09	1.24	1.19	5.80×10^{-1}	1.02×10^1	1.05×10^1	5.86×10^{-4}	6.70×10^{-4}	5.93×10^2	3.03×10^2
No Exploit	3.35	7.60×10^{-1}	1.66	4.23×10^{-1}	1.46×10^1	1.03×10^1	1.93×10^{-3}	2.66×10^{-3}	3.12×10^2	1.88×10^2
AEGiS	2.90	1.44	1.39	5.38×10^{-1}	1.46×10^1	2.95	2.21×10^{-3}	2.77×10^{-3}	4.20×10^2	2.33×10^2

Method	StyblinskiTang7 (7)		Ackley10 (10)		Michalewicz10 (10)		Rosenbrock10 (10)		StyblinskiTang10 (10)	
	Median	MAD	Median	MAD	Median	MAD	Median	MAD	Median	MAD
No PF	3.20×10^1	1.67×10^1	1.82×10^1	1.00	1.07	4.16×10^{-1}	1.51×10^3	9.78×10^2	5.73×10^1	2.04×10^1
No TS	3.92×10^1	1.32×10^1	1.04×10^1	3.56	5.78×10^{-1}	4.85×10^{-1}	1.12×10^3	7.36×10^2	6.31×10^1	2.16×10^1
No Exploit	5.19×10^1	2.51×10^1	7.82	1.52	1.14	5.01×10^{-1}	7.89×10^2	4.23×10^2	1.49×10^2	2.73×10^1
AEGiS	3.07×10^1	1.89×10^1	1.27×10^1	2.38	4.46×10^{-1}	5.98×10^{-1}	1.03×10^3	7.26×10^2	5.95×10^1	2.10×10^1

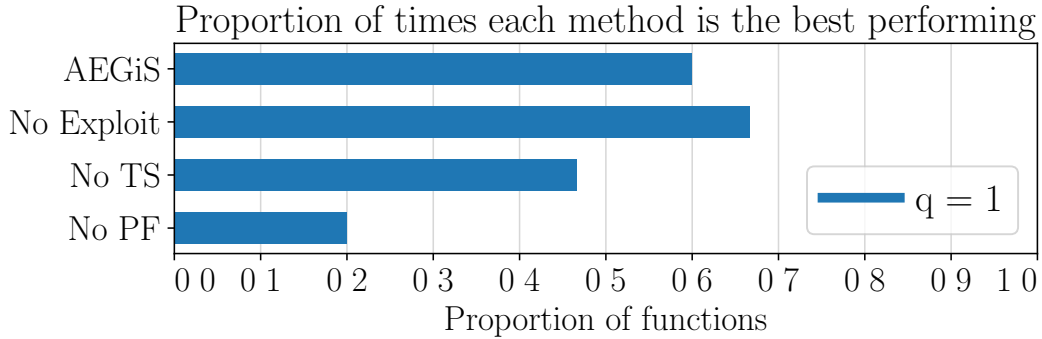
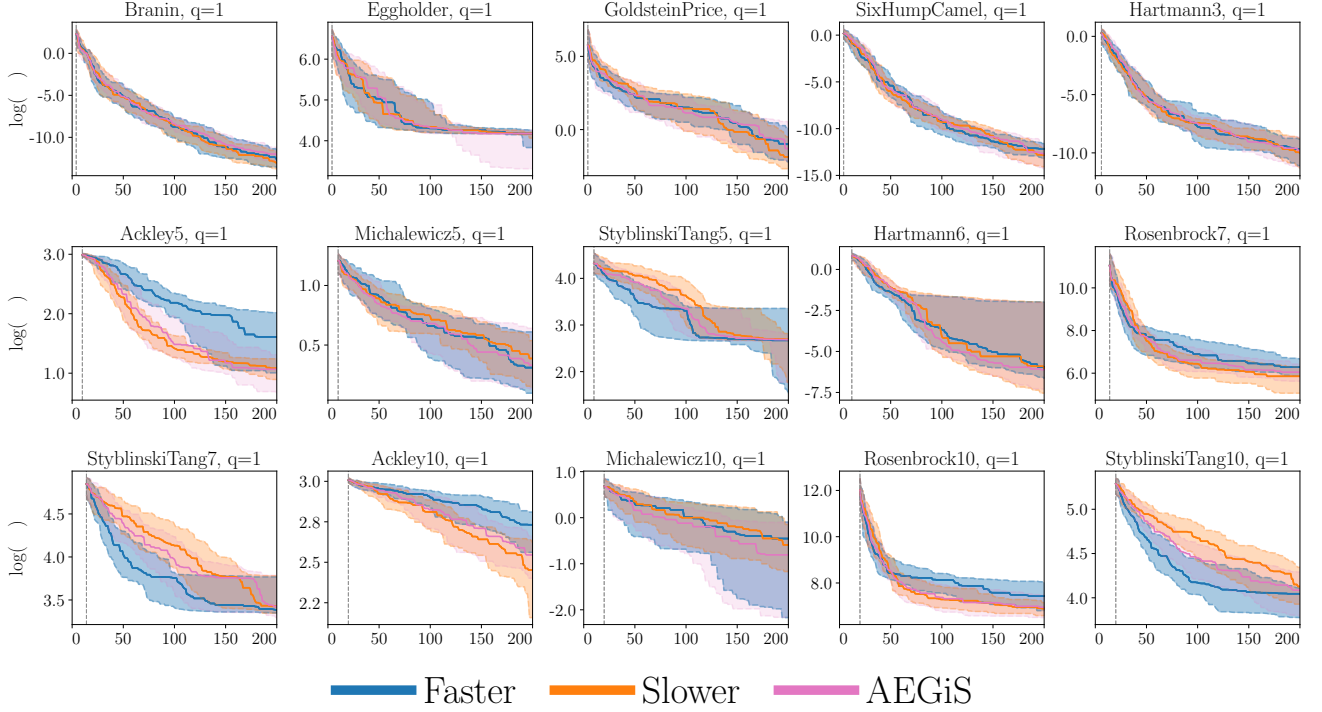


Figure 13: Ablation study summary. Bar lengths correspond to the proportion of times that a method is best or statistically equivalent to the best method across the 15 synthetic functions.

6.3 Setting ϵ

Lastly, we compare different rates of ϵ decay. Here, *faster* corresponds to a quicker rate of decay and thus an increase in exploitation, and *slower* corresponds to a reduced rate, leading to less exploitation. Figure 14 shows the convergence plots for the benchmark functions, with solid lines showing the median log simple regret and shading showing the interquartile range. Table 13, show the median log simple regret as well as the median absolute deviation from the median (MAD), a robust measure of dispersion. The method with the best (lowest) median regret is shown in dark grey, and those that are statistically equivalent to the best method according to a one-sided, paired Wilcoxon signed-rank test with Holm-Bonferroni correction (Holm, 1979) ($p \geq 0.05$) are shown in light grey. Figure 15 summarises the tabulated results and shows the number of times each method is best or statistically equal to the best performing method.

Figure 14: Convergence results for the setting ϵ experiments.Table 13: Tabulated results for the setting ϵ experiments. The table shows the median log simple regret (*left*) and median absolute deviation from the median (MAD, *right*) after 200 function evaluations across the 51 runs. The method with the lowest median performance is shown in dark grey, with those with statistically equivalent performance are shown in light grey.

Method	Branin (2)		Eggholder (2)		GoldsteinPrice (2)		SixHumpCamel (2)		Hartmann3 (3)	
	Median	MAD	Median	MAD	Median	MAD	Median	MAD	Median	MAD
Faster	3.16×10^{-6}	4.21×10^{-6}	6.51×10^1	8.39	3.68×10^{-1}	4.81×10^{-1}	5.28×10^{-6}	5.65×10^{-6}	6.15×10^{-5}	7.50×10^{-5}
Slower	2.23×10^{-6}	2.69×10^{-6}	6.51×10^1	4.03	1.55×10^{-1}	1.84×10^{-1}	2.75×10^{-6}	3.13×10^{-6}	4.44×10^{-5}	6.19×10^{-5}
AEGiS	5.69×10^{-6}	4.87×10^{-6}	6.51×10^1	2.09×10^1	2.71×10^{-1}	3.67×10^{-1}	3.08×10^{-6}	3.94×10^{-6}	5.62×10^{-5}	6.94×10^{-5}
Method	Ackley5 (5)		Michalewicz5 (5)		StyblinskiTang5 (5)		Hartmann6 (6)		Rosenbrock7 (7)	
	Median	MAD	Median	MAD	Median	MAD	Median	MAD	Median	MAD
Faster	5.00	3.62	1.36	5.55×10^{-1}	1.45×10^1	2.03×10^1	2.59×10^{-3}	2.83×10^{-3}	5.34×10^2	3.07×10^2
Slower	2.95	7.71×10^{-1}	1.47	4.00×10^{-1}	1.47×10^1	3.93	2.45×10^{-3}	3.39×10^{-3}	3.49×10^2	2.82×10^2
AEGiS	2.90	1.44	1.39	5.38×10^{-1}	1.46×10^1	2.95	2.21×10^{-3}	2.77×10^{-3}	4.20×10^2	2.33×10^2
Method	StyblinskiTang7 (7)		Ackley10 (10)		Michalewicz10 (10)		Rosenbrock10 (10)		StyblinskiTang10 (10)	
	Median	MAD	Median	MAD	Median	MAD	Median	MAD	Median	MAD
Faster	2.95×10^1	1.98×10^1	1.54×10^1	3.28	6.36×10^{-1}	7.34×10^{-1}	1.69×10^3	1.44×10^3	5.71×10^1	2.00×10^1
Slower	3.08×10^1	1.87×10^1	1.16×10^1	3.73	5.54×10^{-1}	4.15×10^{-1}	9.86×10^2	3.87×10^2	6.20×10^1	2.15×10^1
AEGiS	3.07×10^1	1.89×10^1	1.27×10^1	2.38	4.46×10^{-1}	5.98×10^{-1}	1.03×10^3	7.26×10^2	5.95×10^1	2.10×10^1

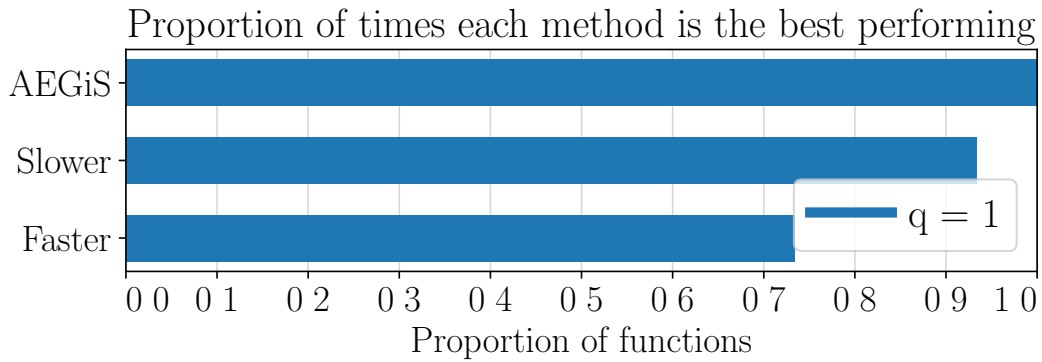


Figure 15: Setting ϵ summary. Bar lengths correspond to the proportion of times that a method is best or statistically equivalent to the best method across the 15 synthetic functions.

References

- Deb, K., Pratap, A., Agarwal, S., and Meyarivan, T. (2002). A fast and elitist multiobjective genetic algorithm: NSGA-II. *IEEE Transactions on Evolutionary Computation*, 6(2):182–197.
- Holm, S. (1979). A simple sequentially rejective multiple test procedure. *Scandinavian Journal of Statistics*, 6(2):65–70.
- Klein, A., Dai, Z., Hutter, F., Lawrence, N., and Gonzalez, J. (2019). Meta-surrogate benchmarking for hyperparameter optimization. In *Advances in Neural Information Processing Systems 32*, pages 6270–6280. Curran Associates, Inc.